NEW TECH I NEW CARE

EVIDENCE PAPERS

www.xyz-life.com

XYZlife Patch BC1product features are based on scientific research and journal published. It is a complete and reliable product.

1. Arrhythmia Evaluation in Wearable ECG Devices
2. Predicting the Percentage of Atrial Fibrillation using Sample Entropy
3. A Modular Integrating Algorithm for Multiple Arrhythmia Detection
4. A Threshold-based Algorihum of Fall Detection Using a Wearable Device with Tri-axial Accelerometer and Gyroscope
5. An Effective Algorithm for Dynamic Pedometer Calculation

1.

Arrhythmia Evaluation in Wearable ECG Devices

sensors

MDPI

Article

Arrhythmia Evaluation in Wearable ECG Devices

Muammar Sadrawi [1], Chien-Hung Lin [2], Yin-Tsong Lin [2], Yita Hsieh [2], Chia-Chun Kuo [2], Jen Chien Chien [2], Koichi Haraikawa [2], Maysam F. Abbod [3] and Jiann-Shing Shieh [1,*]

1 Department of Mechanical Engineering and Innovation Center for Big Data and Digital Convergence, Yuan Ze University, Taoyuan, Chung-Li 32003, Taiwan; muammarsadrawi@yahoo.com
2 Healthcare and Beauty RD Center, Kinpo Electronics, Inc., New Taipei City 222, Taiwan; lance_lin@kinpo.com.tw (C.-H.L.); lotusytlin@calcomp.com.tw (Y.-T.L.); yita_hsieh@calcomp.com.tw (Y.H.); cckuo@calcomp.com.tw (C.-C.K.); jcchien@kinpo.com.tw (J.C.C.); koichi_h@kinpo.com.tw (K.H.)
3 Department of Electronic and Computer Engineering, Brunel University London, Uxbridge UB8 3PH, UK; Maysam.Abbod@brunel.ac.uk
* Correspondence: jsshieh@saturn.yzu.edu.tw

Received: 19 September 2017; Accepted: 21 October 2017; Published: 25 October 2017

Abstract: This study evaluates four databases from PhysioNet: The American Heart Association database (AHADB), Creighton University Ventricular Tachyarrhythmia database (CUDB), MIT-BIH Arrhythmia database (MITDB), and MIT-BIH Noise Stress Test database (NSTDB). The ANSI/AAMI EC57:2012 is used for the evaluation of the algorithms for the supraventricular ectopic beat (SVEB), ventricular ectopic beat (VEB), atrial fibrillation (AF), and ventricular fibrillation (VF) via the evaluation of the sensitivity, positive predictivity and false positive rate. Sample entropy, fast Fourier transform (FFT), and multilayer perceptron neural network with backpropagation training algorithm are selected for the integrated detection algorithms. For this study, the result for SVEB has some improvements compared to a previous study that also utilized ANSI/AAMI EC57. In further, VEB sensitivity and positive predictivity gross evaluations have greater than 80%, except for the positive predictivity of the NSTDB database. For AF gross evaluation of MITDB database, the results show very good classification, excluding the episode sensitivity. In advanced, for VF gross evaluation, the episode sensitivity and positive predictivity for the AHADB, MITDB, and CUDB, have greater than 80%, except for MITDB episode positive predictivity, which is 75%. The achieved results show that the proposed integrated SVEB, VEB, AF, and VF detection algorithm has an accurate classification according to ANSI/AAMI EC57:2012. In conclusion, the proposed integrated detection algorithm can achieve good accuracy in comparison with other previous studies. Furthermore, more advanced algorithms and hardware devices should be performed in future for arrhythmia detection and evaluation.

Keywords: wearable sensor; arrhythmia; sample entropy; fast Fourier transform; artificial neural networks

1. Introduction

Nowadays, wearable sensor-based system has been applied to wide applications. Fall and activity monitoring study with utilizing wearable sensor has been conducted by Shany et al. [1]. This kind of system was also used for Parkinson's disease with the combination of Support Vector Machine (SVM) by a study conducted by Patel et al. [2]. Meanwhile, Corbishley et al. used non-invasive and continuous wearable system for breathing monitoring [3]. Furthermore, wearable electrocardiogram (ECG) device was also utilized for the emotion classifications via hear rate variability [4].

Recently, the implementation of intensively evaluated ECG signal through wearable sensor is one of the essential issues for the cardiovascular-related diseases. For example, arrhythmia has been one of

the concerning cardiac diseases. Some of the arrhythmia cases are classified as life-threatening events. Therefore, Rosenberg et al. utilized long-term monitoring system for atrial fibrillation monitoring [5]. A study by Baig et al. evaluated wearable ECG system for older-adult population [6]. Furthermore, Fensli et al. utilized wearable sensor for arrhythmia detection applied to tele-home care system via general packet radio service (GPRS) to personal computer as base station. This information will be evaluated by doctors with remote system for the rhythm evaluation by the internet connection server [7]. Lin et al. developed an intelligent telecardiology system for sinus tachycardia, sinus bradycardia, wide QRS complex, atrial fibrillation, and cardiac asystole [8]. This system can also activate emergency alarm. In advanced, Hu et al. had successfully applied hidden Markov model to using wearable system for ECG arrhythmia evaluation [9]. Meanwhile, recent study by Hadiyoso et al. also conducted a study on arrhythmia detection via smart phone [10].

Atrial fibrillation (AF) and ventricular fibrillation (VF) are frequent arrhythmias. The former, AF, is one of the arrhythmias related to age and has serious effect on morbidity, mortality, and cost [11]. AF also is an independent factor and has significant effect on the risk of stroke by a study conducted by Wolf et al. on five thousand cases both female and male for more than thirty years [12]. Kara et al. utilized power spectral density and Daubechies wavelets with backpropagation artificial neural network (ANN) for AF detection [13]. Roonizi et al. used extended Kalman filter to evaluate AF frequency [14]. A study by Mohebbi et al. investigated AF by applying the feature dimension reduction technique with SVM classifier [15]. Abdul-Kadir et al. used dynamic ECG system according to second order differential equation of ECG behavior with cross validation technique by utilizing SVM and ANN as predictors [16]. Recently, Rajpurkar et al. have utilized one of the deep learning techniques, namely a 34-layer convolutional neural network for detecting arrhythmia, including AF [17].

Another arrhythmia is VF. According to McWilliam, VF has strong correlation with sudden cardiac diseases [18] and it is critical to defibrillation [19]. Alonso-Atienza et al. have applied bootstrap resampling-based feature extraction SVM classifier for VF detection [20]. A study by Anas et al. describes how empirical mode decomposition method is used to discriminate VF and non-VF rhythms [21].

Atrial premature complex (APC) and ventricular premature complex (VPC) are other frequent arrhythmias that, according to the ANSI/AAMI EC57:2012, can be classified as supraventricular ectopic beat (SVEB) and ventricular ectopic beat (VEB). Research on detecting these conditions and other arrhythmias have been in several previous studies. Thong et al., have utilized paroxysmal atrial fibrillation for APC calculation [22]. Sayadi et al. have used extended Kalman filter for VPC detection [23]. Similarly, a study by Özbay et al. that evaluated the performance of the neural networks also performed the initialization of fuzzy C-means for APC, VPC, and other ECG arrhythmia [24]. Song et al. utilized support vector machine with the combination of dimensionality reduction using principal component analysis, and linear discriminant analysis for arrhythmia classifier including APC and VPC. They found better result as compared to multilayer perceptron (MLP) and fuzzy inference system [25].

However, these previous studies are relatively computationally complex to be applied to wearable devices. Several studies, which are relatively less computational complexity, performed well for AF and VF detection. For AF detection, Zhou et al. proposed a powerful algorithm for real time detection of AF. This study evaluated the heart rate to create a symbolic and word sequences. In advanced, Shannon entropy was utilized to evaluate the word sequence in order to classify AF [26]. On the other hand, FFT algorithm has been a robust algorithm for signal detection algorithm in recent studies [27–30] and has been effectively applied for VF detection for decades. For VF, Clayton et al. evaluated signal spectrum by utilizing fast Fourier transform (FFT) and maximum entropy for VF detection [31]. Afonso et al. applied short time Fourier transform (STFT), smoothed pseudo Wigner-Ville distribution and cone-shaped kernel for the VF evaluation [32]. Recently, wearable sensor-based system has been widely applied and utilized, the chance of the real-time evaluation for the arrhythmia detection with the less-complicated algorithms is highly likely an acceptable investigation. Hence, the main purpose

of this study is to efficiently apply less complexity algorithms for real-time detection of arrhythmias utilizing wearable devices based on ANSI/AAMI EC57:2012 evaluation.

2. Materials and Methods

For the hardware part, BC1 ECG device (Bio Clothing One, XYZ life BC1, Kinpo Inc., Taipei, Taiwan) single lead heart rate monitor front end is ADI ADS 8232 (Analog Devices, Inc., Norwood, MA, USA). The BC1 ECG device uses wet electrode. The detail of the BC1 ECG device is shown in Figure 1. Meanwhile, its specification is shown in Table 1. This device is configured by 0.5 Hz two-pole high-pass filter and two-pole 40 Hz for the low-pass filter [33]. For the micro controller unit (MCU), Texas Instruments MSP430 series is selected to have an ultra-low power unit that has 128 KB flash ROM and 8 kB SRAM. This unit is a 16-bit reduced instruction set computer (RISC) architecture of up to 25 MHz system clock with 12-bit analog-to-digital converter (ADC). In further, the Bluetooth low energy (BLE) using Texas Instruments CC25 series (Texas Instruments Incorporated, Dallas, 75243 TX, USA) connection system is utilized to have a power-optimized system-on-chip (SOC) solution that supports maximum 2 Mbps data rates. The small start button powers the device on. The device will detect the connection of the Bluetooth, which will either associate the smartphone or not. When there is no Bluetooth device connection, the device will be turned to off-line state allowing the data to be stored only in the SD card. Meanwhile, the on-line evaluation will send real-time ECG data to the smartphone application for the arrhythmia classification.

This study uses PhysioNet database [34] for algorithm development and testing. Furthermore, simulator data from Fluke ProSim 8 vital sign patient monitor simulator (Fluke Biomedical Division of Fluke Electronics Corporation, Everett, 98203 WA, USA) is conducted for real-time detection. The four databases provided by PhysioNet are American Heart Association database (AHADB), Creighton University Ventricular Tachyarrhythmia database (CUDB) [34,35], MIT-BIH Arrhythmia database (MITDB) [34,36], and MIT-BIH Noise Stress Test database (NSTDB) [34,37]. For SVEB (i.e., APC) classification, 44 records for MITDB is analyzed. Meanwhile for VEB (i.e., VPC) detection, 78 records for AHADB, 44 records for MITDB, and 12 records for NSTDB are used in the evaluation. For AF detection, 44 records for MITDB are utilized for the evaluation. Furthermore, 78 records for AHADB, 44 records for MITDB, and 35 records for CUDB are used for VF classification. Evaluation of sensitivity (Se), positive predictivity (+P), and false positive rate (FPR) are defined for the evaluation performance of SVEB (i.e., APC) and VEB (i.e., VPC). Meanwhile, episode sensitivity (ESe), episode positive predictivity (E + P), duration sensitivity (DSe), and duration positive predictivity (D + P) are utilized for AF and VF detections. All of the evaluations are performed according to ANSI/AAMI EC57:2012 [38].

For simulation and visualization in smartphone for real-time application, Fluke ProSim 8 is also utilized. Simulation data includes several ECG rhythms: normal sinus rhythm, APC, VPC, AF, and VF signals in real-time situation and evaluation on the smartphone. Initially, simulation data from Fluke simulator is transferred to BC1. Programming of the arrhythmia algorithm is conducted in Java (Android) and Objective-C (iOS). The performance of this algorithm is evaluated by WFDB (WaveForm DataBase) software on Windows acquired from PhysioNet.

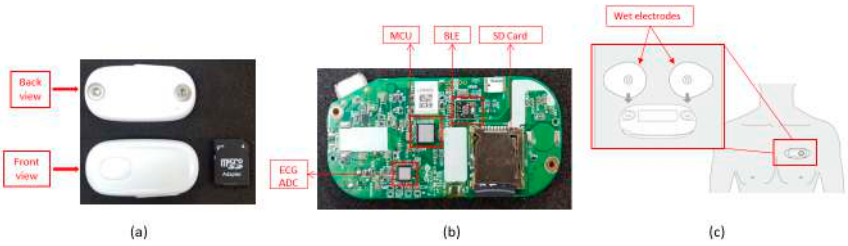

Figure 1. The BC1 electrocardiogram (ECG) device: (**a**) Front and back views; (**b**) Processing, transmitting and saving units detail; and, (**c**) Position with the electrodes.

Table 1. The BC1 device specification.

CMRR (Common-mode rejection ratio)	80 dB (dc to 60 Hz)
High signal gain	(G = 100) with dc blocking capabilities
Single-supply operation	2.0 V to 3.5 V
ADC (Analog-to-Digital Converter)	12-bit
Input Impedance	5 Giga Ohm

The integrated evaluation is started by evaluating the APC, VPC, AF, and VF based on ANSI/AAMI EC57:2012, as shown in Figure 2. Originally, the data downloaded from PhysioNet [34–37] is downsampled to 200 Hz. Initially the 5-min ECG signal is evaluated either based on the beat, for VPC, AF, and APC evaluations or the raw ECG signal, the 2-s window, for VF detection.

VPC evaluation is initiated by the R-R interval evaluation. The evaluation is calculated based-on the study by Hamilton et al. [39]. Another study by Hamilton [40] is utilized for VPC evaluation, as shown on Figure 2A. For AF calculation, the previous evaluation of VPC beat is essentially important. The abnormal beats (i.e., VPC beats) will imitate the R-R interval in the normal rhythm. This phenomenon highly likely increases the uncertainty in classifying either normal or AF rhythm. Previous classification results for detecting VPC will be utilized to reform the original R-R interval by averaging the previous beat and the next beat. The AF evaluation is originally calculated based on Zhou et al. study [26]. The heart rate is calculated from the original R-R interval. This heart rate is converted to symbolic sequence using Equation (1). Furthermore, this symbolic sequence is utilized for the word value by Equation (2) as shown by the following:

$$sy_n = \begin{cases} 63 & if\ hr_n \geq 315 \\ \lfloor hr_n/5 \rfloor & other\ cases \end{cases} \quad (1)$$

$$wv_n = \left(sy_{n-2}\ x\ 2^{12}\right) + \left(sy_{n-1}\ x\ 2^{6}\right) + sy_n \quad (2)$$

where hr is the heart rate, sy_n is the symbolic sequence, and wv_n is the word value. This word value sequence evaluation, originally calculated using Shannon entropy, is replaced by sample entropy algorithm [41]. AF evaluation can be seen in Figure 2B.

For APC detection, the morphological ECG is utilized for feature extraction and artificial neural networks. Multi-layer perceptron with backpropagation training algorithm and single hidden layer is utilized. Features for the ANN input extracted from ECG signal are P-R interval, QRS duration, R-R interval, next R-R interval, average, and standard deviation of R-R interval of 10 beats before and after the current beat, and R-wave amplitude, as shown in Figures 2C and 3, which is based on our previous study [42]. The data is divided into 60% for training, 20% for validation, and 20% for testing.

After R-R interval-based algorithm is performed, the raw ECG signal-based evaluation is calculated. The initial 5-min ECG segment is reshaped to several 2-s ECG signals. This evaluation is organized to avoid mixed rhythms for the classification. The periodogram evaluation is utilized by finding its maximum point corresponding to the frequency of the shortened ECG segments. According to Lo et al., the dominant VF waveform frequency is between 1 Hz and 7 Hz [43]. Our study utilizes a similar range with some offset. Three focused area of maximas are defined. The first one is the VF area (p_vf). This area is located in between the frequency of greater than equals to 2.61 Hz and less than equals to 4.95 Hz. The next area is the first area of non-VF (p_nVF), which is between frequency greater than 0.5 Hz and less than 2.61 Hz. The last area is the second non-VF (p_nVF2), which is located between frequency greater than 4.95 Hz and less than or equals to 10 Hz. The ratio of the p_vf to the summation of the p_nVF and p_nVF2 is defined in order to classify either normal or VF rhythm. The threshold of the ratio is fixed to 3.96. The detailed evaluation of the VF arrhythmia can be seen in Figure 2D.

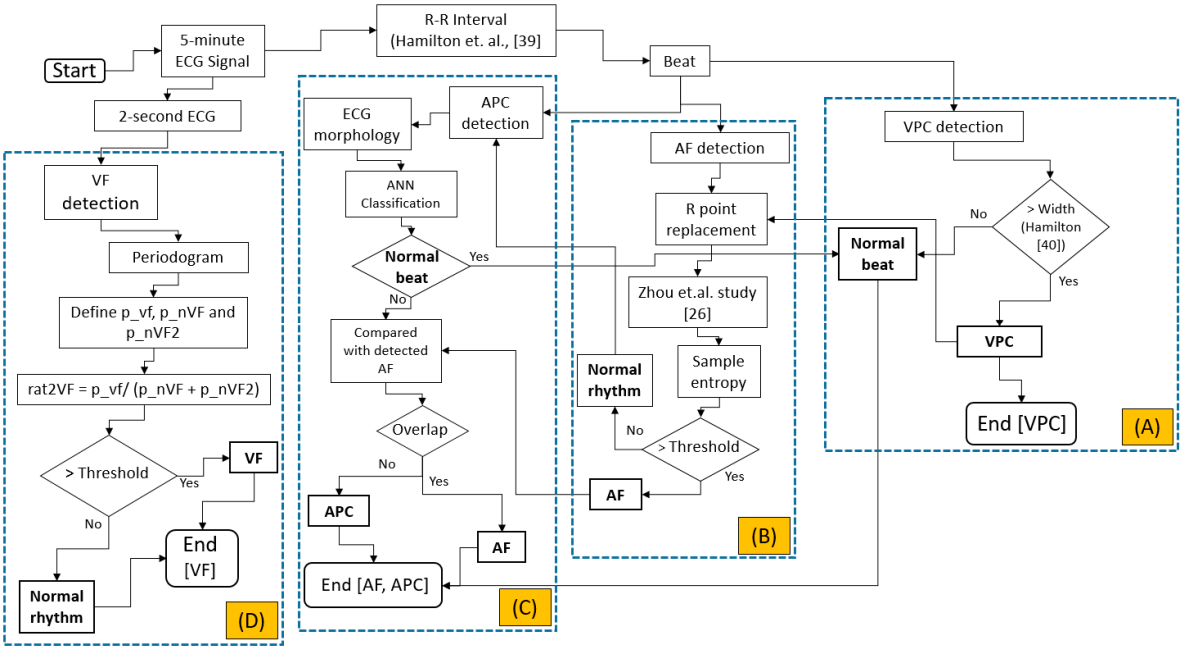

Figure 2. Integrated arrhythmia evaluation flowchart; (**A**) Ventricular premature complex detection; (**B**) Atrial fibrillation detection; (**C**) Atrial premature complex detection; (**D**) Ventricular fibrillation detection.

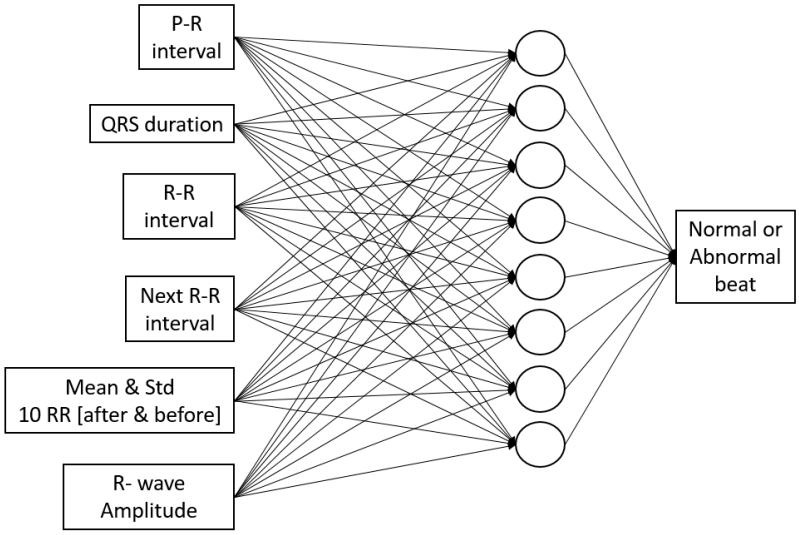

Figure 3. Artificial neural network (ANN) structure for detecting normal or abnormal beat in APC detection algorithm.

3. Results

Prior to PhysioNet database evaluation, Fluke simulator data of Normal sinus rhythm, APC, VPC, AF, and VF are utilized from BC1 for algorithm evaluation on smartphone in real-time condition. Besides, visualizing real-time signals with its signal annotation are shown in Figure 4. For APC and VPC, detection is evaluated based-on the R-wave of the ECG signal. Meanwhile, normal sinus rhythm, AF and VF evaluation works based-on a segment. The mobile application is also able to store the documented signal with its signal annotation as the off-line evaluation records that can be seen in Figure 5.

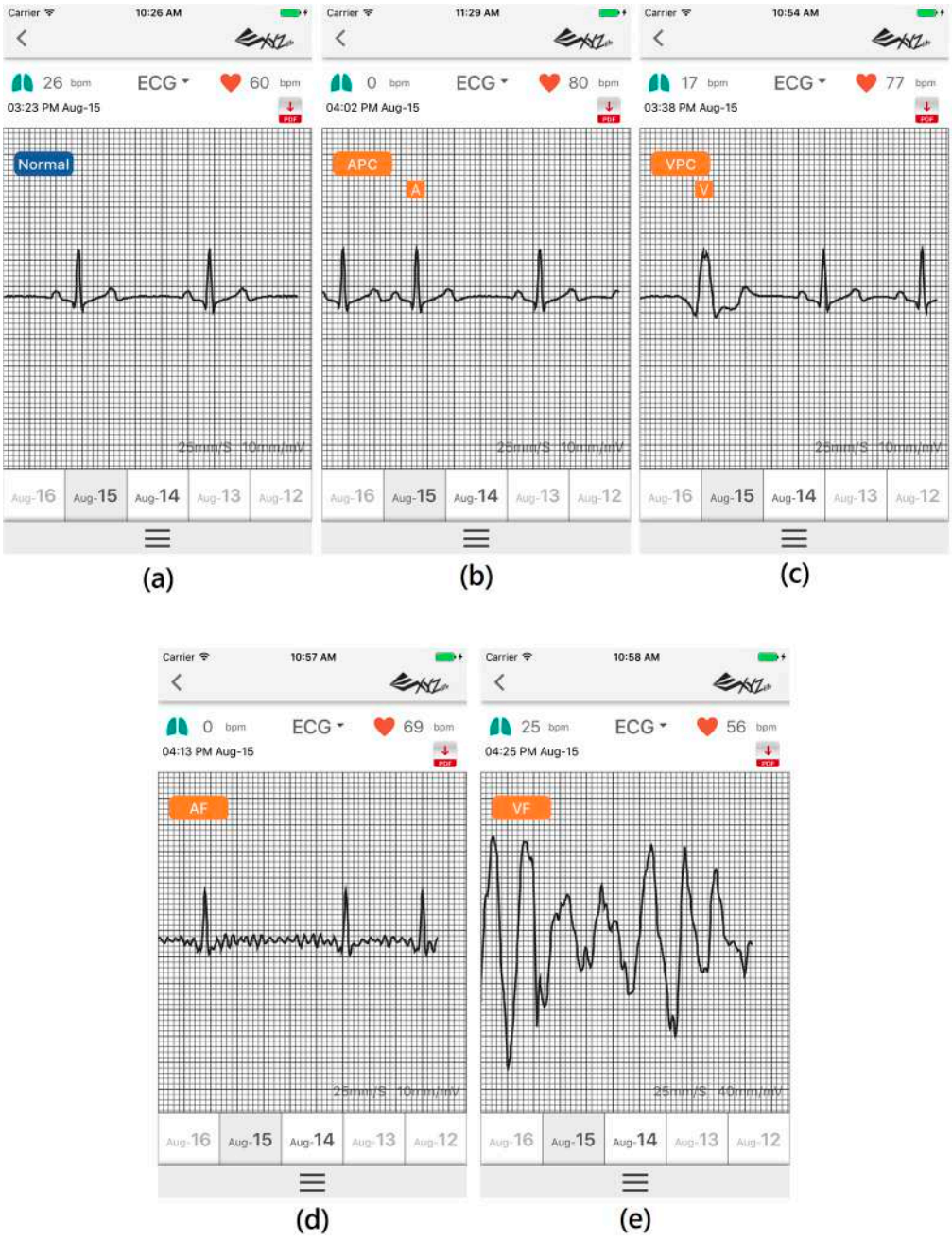

Figure 4. Simulation result from Fluke simulator displayed on mobile phone; (**a**) Normal sinus rhythm; (**b**) Atrial Premature Complex (APC); (**c**) Ventricular Premature Complex (VPC); (**d**) Atrial fibrillation; and, (**e**) Ventricular fibrillation.

The entire evaluation of arrhythmia can be seen in Tables 2 and 3. For SVEB (i.e., APC) evaluation utilizing the MITDB database, the performances are 79.87%, 67.14%, and 1.323%, respectively, for the gross evaluation of Se, +P and FPR. Meanwhile for the average evaluation, Se, +P and FPR are 71.35%, 36.9%, and 2.098%, respectively.

The next evaluation is VEB (i.e., VPC). For this evaluation, utilizing a study by Hamilton [38], the gross evaluation from AHADB for Se, +P and FPR are 89.75%, 96.08%, and 0.371%, respectively. For average evaluation, Se, +P and FPR are 86.52%, 84.67%, and 0.458%. For MITDB database, the algorithm performances are 93.10%, 95.65% and 0.321% for gross evaluation of Se, +P, and FPR, respectively. Average evaluation has Se, +P, and FPR by 87.27%, 73.26%, and 0.336%, respectively.

The third database for the VEB evaluation utilizes the NSTDB database. The performance for this database for gross evaluation respectively for the Se, +P and FPR are 83.22%, 45.79% and 10.180%. The average evaluation has 58.17%, 50.86% and 9.032% respectively Se, +P and FPR.

The next evaluation is for AF and VF rhythms. AF performance evaluation is calculated using MITDB database. For the gross evaluation, the performances are 62%, 100%, 92%, and 92% for ESe, E + P, DSe, and D + P, respectively. The average evaluations for ESe, E + P, DSe, and D + P, are 70%, 100%, 85%, and 86%.

The next evaluation is VF detection. This evaluation starts using AHADB database. For the gross evaluation, performances are 90%, 95%, 28%, and 97% for ESe, E + P, DSe, and D + P, respectively. Average evaluations for ESe, E + P, DSe, and D + P are 94%, 69%, 33%, and 70%. The second database used for VF evaluation is MITDB database. The gross evaluations are 100%, 75%, 69%, and 88% for ESe, E + P, DSe, and D + P, respectively. For average evaluation, it is 100%, 33%, 69%, and 33% for ESe, E + P, DSe, and D + P, respectively. The last database utilized for VF evaluation is CUDB. For this database, the gross evaluations are 83%, 90%, 32%, and 94% for ESe, E + P, DSe, and D + P, respectively. Meanwhile, for average evaluation it is 84%, 83%, 40%, and 84%, for ESe, E + P, DSe, and D + P, respectively.

Table 2. The entire supraventricular ectopic beat (SVEB) (i.e., APC) and ventricular ectopic beat (VEB) (i.e., VPC) evaluation result. (* = exclude records 2202, 8205; ** = exclude records 102, 104, 107, 217; N/A: not available. Se = Sensitivity, +P = Positive predictivity and FPR = False positive rate).

Database	Statistics	SVEB			VEB		
		Se	+P	FPR	Se	+P	FPR
AHADB *	Gross	N/A	N/A	N/A	89.75	96.08	0.371
	Average	N/A	N/A	N/A	86.52	84.67	0.458
MITDB **	Gross	79.87	67.14	1.323	93.10	95.65	0.321
	Average	71.35	36.9	2.098	87.27	73.26	0.336
NSTDB	Gross	N/A	N/A	N/A	83.22	45.79	10.180
	Average	N/A	N/A	N/A	58.17	50.86	9.032

Table 3. The entire atrial fibrillation (AF) and VF evaluation result. (* = exclude records 2202, 8205; ** = exclude records 102, 104, 107, 217; N/A: not available. ESe = Episode sensitivity, E + P = Episode positive predictivity, DSe = Duration sensitivity, D + P = Duration positive predictivity).

Database	Statistics	AF				VF			
		ESe	E + P	DSe	D + P	ESe	E + P	DSe	D + P
AHADB *	Gross	N/A	N/A	N/A	N/A	90	95	28	97
	Average	N/A	N/A	N/A	N/A	94	69	33	70
MITDB **	Gross	62	100	92	92	100	75	69	88
	Average	70	100	85	86	100	33	69	33
CUDB	Gross	N/A	N/A	N/A	N/A	83	90	32	94
	Average	N/A	N/A	N/A	N/A	84	83	40	84

Figure 5. Documented simulation results from Fluke simulator; (**a**) Normal sinus rhythm; (**b**) Atrial Premature Complex (APC); (**c**) Ventricular Premature Complex (VPC); (**d**) Atrial fibrillation and (**e**) Ventricular fibrillation.

4. Discussion

This study evaluates several arrhythmias, SVEB (i.e., APC), VEB (i.e., VPC), AF, and VF, based-on ANSI/AAMI EC57:2012 of totally 169 records from three PhysioNet databases with applying less computationally complicated algorithms. The performances of the algorithms are evaluated based-on the sensitivity, positive predictivity, and false positive rate. The applied methods utilized in this study are relatively less complex; namely sample entropy, FFT, and the ANN. For ANN, the features extracted from ECG signal are also acceptable in the feedforward run. This condition has purposed to minimize the computational time, while performing testing in the real-time application.

In order to study the measurement evaluation of previous studies conducted based-on ANSI/AAMI EC57, the results are compared to our results as shown on Table 4 for SVEB and VEB results. For SVEB and VEB, a study conducted by De Chazal et al. [44] is investigated. This study showed that SVEB evaluation produced gross evaluation of Se, +P and FPR as 75.9%, 38.5%, and 4.7%,

respectively. For comparison purposes, we found that our study has better performances with respect to gross evaluation of Se, +P and FPR, which are 79.87%, 67.14%, and 1.323%, respectively. For VEB classification, De Chazal et al. [44] has gross evaluation of Se, +P and FPR are 77.7%, 81.9%, and 1.2%. Meanwhile, with utilizing a study by Hamilton [40], our results also showed better achievement by producing 93.1%, 95.65%, and 0.321%, respectively, for gross evaluation of Se, +P and FPR.

Table 4. The SVEB (i.e., APC) and VEB (i.e., VPC) result comparison.

	Sensitivity (%)		Positive Predictivity (%)		False Positive Rate (%)	
	This Study	De Chazal et al. [44]	This Study	De Chazal et al. [44]	This Study	De Chazal et al. [44]
SVEB	79.87	75.9	67.14	38.5	1.323	4.7
VEB	93.1	77.7	95.65	81.9	0.321	1.2

For AF study, results are compared with a previous study conducted by Young et al. [45]. This study performed hidden Markov model (HMM) evaluation using ANSI/AAMI:EC57 for evaluation. Twelve MIT-BIH Arrhythmia database records were utilized for training. Furthermore, for testing data, MIT-BIH AF database was used. In order to perform a comparison to this study, only training results from Young et al. study are investigated. From the results of Young et al. study, a sensitivity evaluation provides a better result of 97.7% as compared to this study evaluating 44 MIT-BIH Arrhythmia database records for ESe that has 62%, and DSe that has 92% for gross statistics evaluations. However, this study produces better results for both E + P that has 100%, and D + P that has 92% for gross statistics evaluations in comparison to their study, which resulted in 86.77% for the positive predictivity.

For a VF comparison study, studies by Park et al. [46] and Moraes et al. [47] are utilized. A study by Park et al. evaluated AHADB and MIT-BIH arrhythmia databases by applying decision rule-based algorithm and utilizing ANSI/AAMI:EC57. This study has evaluated the duration sensitivity and duration positive predictivity. For AHADB evaluations, a study by Park et al., utilized 11 records from AHADB, have 98.1% and 99.1%, respectively, for the DSe and D + P results. Meanwhile, our study, evaluating 78 records from AHADB, for DSe and D + P produces 28% and 97%, respectively for gross statistics evaluations. Furthermore, for MIT-BIH arrhythmia database evaluation, a study by Park et al., evaluated only record 207, has 88.5% and 86.3% for DSe and D + P, respectively. Hence, this study, utilizing 44 records, has achieved 69% and 88% for DSe and D + P, respectively.

Another study is performed for the purpose of VF evaluation comparison. Moraes et al. [47] conducted a study by combining two algorithms, VF filter leakage and complexity measure algorithms. This study has also utilized ANSI/AAMI:EC57 for the evaluation of CUDB. The combined algorithm by Moraes et al. study provided sensitivity and positive predictivity evaluations, by utilizing 30 records. For comparison study purposes, our results, utilizing 35 records, have 83% for ESe and 32% for DSe gross statistics evaluations. Meanwhile, a study by Moraes et al. has 70.32% for the sensitivity. In addition, the results of this study have 90% for E + P and 94% for D + P gross statistics evaluations. However, study by Moraes et al. has 94.66% positive predictivity. The overall comparison of the PhysioNet-based database for the AF and VF can be seen by Table 5.

The evaluation of AF evaluation in the wearable ECG device is compared to study by Lin et al. [8]. This study applied the expert system algorithm. A three-lead ECG device with 512 Hz sampling frequency and 12-bit resolution was utilized for 10 normal and 20 AF patients. For the evaluation, the 12-lead ECG system result was investigated by the cardiologists. The sensitivity and the positive predictive performance are 94.56% and 99.39%, respectively. For the comparison, Lin et al. study performed better accuracy than our study. However, our study evaluates the episode and duration separately according to ANSI/AAMI:EC57 for the sensitivity and positive predictivity.

For computational time, a study by Chakroborty et al. is utilized for the comparison [48]. This study proposed a solution for the arrhythmia classifications. The classified arrhythmias are normal, left bundle branch block (LBBB), right bundle branch block (RBBB), PVC, and PAC. The MIT-BIH

Arrhythmia database was utilized for the evaluation. This study provided the overall evaluation time is 6875.3 s. For this study in computational time evaluation, the personal computer (PC), and smartphone-based computational time are evaluated. The PC specification is MacBook Air, Intel Core i5, and 1.6 GHz. Meanwhile, the smartphone is iPhone 5S, A7 chip, 64-bit architecture, and 1.3 GHz frequency. The results show that the computational time for the PC-based calculation is about 174.802 s. Luckily, smartphone-based calculation produces 1840.791 s. The evaluation time in PC and smartphone for MIT-BIH Arrhythmia database can be seen in Table 6. On average, the PC-based computational is 3.591 s and the smartphone-based takes 41.836 s. Meanwhile, our proposed study has been shown less computational time, as shown in Table 7. However, this comparison may not be fully acceptable due to the comparison of LBBB and RBBB detections versus with AF and VF evaluations.

There are several limitations of this study. The first comes from the sliding window for detecting AF. In this study evaluation using sample entropy needs a huge number of the R-R interval. This condition makes delay for the evaluation. However, according to Logan et al., the 5-min sliding window is an acceptable wait for AF detection cases [49].

The second one, ideally, the evaluation of AF and VF should be performed at the same time. However, AF evaluation is performed based-on RR interval and VF evaluation, which is based-on raw ECG signal, these conditions will affect one another. For AF, when evaluation follows VF detection using the raw ECG segment, it will be in an RR shortage condition for the evaluation. Meanwhile, for VF, when the evaluation follows the AF detection (i.e., the R-R interval-based calculation), it highly likely mixes some rhythms inside the calculation window.

The next limitation is the algorithm sequence. Due to our study placing VF detection as the last evaluation, it may appear that VF wave and signal that is close to its wave are similar to the QRS complex classified as VPC class, as shown in Figure 6. This disadvantage is highly likely to be one of the factors negatively affecting VF detection.

For SVEB (i.e., APC) detection, according to ANSI/AAMI EC57, the evaluation should cover all data records. This condition will make a requirement to evaluate not only testing and validation data, but also training data of the ANN, which is learnt by the model in the training.

The device also has several limitations. For this system, the microcontroller unit speed is up to 25 MHz and the Bluetooth module will only support the data transferring maximum 2 Mbps data rates. In this study, utilizing single lead evaluation, these MCU and BLE still work very well. However, these conditions will make our device highly likely to have a problem for the multi-lead ECG signal evaluation.

For the electrode, this study utilizes a wet-based electrode. This electrode may have some disadvantages for the long-term user. The dry-up [50] and sweating [51] may affect the quality of the signal. In further, the utilization of the dry electrode will generate solutions for the wet electrode limitations in biopotential-based evaluation [52–55]. The dry electrode will be one of the future works for our study.

Table 5. The AF and VF result comparison. (N/A = not available).

Arrhythmia	Studies	Database	Number of Data	Evaluation					
				Gross Statistics				Se	+P
				ESe	E + P	DSe	D + P		
Atrial Fibrillation	Proposed study	MITDB	44	62	100	92	92	N/A	N/A
	Young et al. [45]		12	N/A	N/A	N/A	N/A	97.7	86.77
Ventricular Fibrillation	Proposed study	AHADB	78	90	95	28	97	N/A	N/A
	Park et al. [46]		11	N/A	N/A	98.1	99.1	N/A	N/A
	Proposed study	MITDB	44	100	75	69	88	N/A	N/A
	Park et al. [46]		1	N/A	N/A	88.5	86.3	N/A	N/A
	Proposed study	CUDB	35	83	90	32	94	N/A	N/A
	Moraes et al. [47]		30	N/A	N/A	N/A	N/A	70.32	64.66

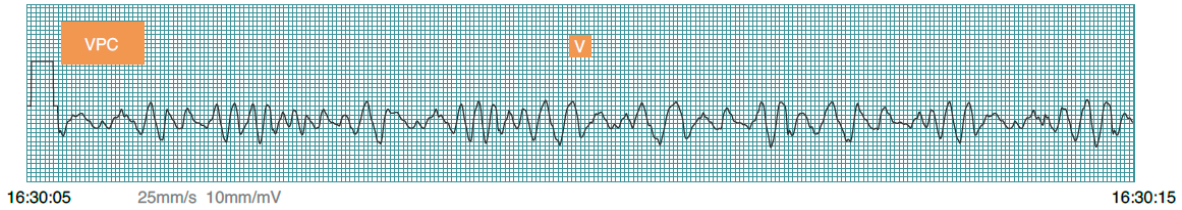

Figure 6. The misclassified VF rhythm to a VPC beat.

Table 6. The proposed integrated algorithm evaluation time in PC and smartphone for the MIT-BIH Arrhythmia database.

Record	Smartphone (s)	PC (s)	Record	Smartphone (s)	PC (s)
100	40.975	3.638	203	41.699	3.891
101	40.964	3.508	205	43.084	4.167
103	41.256	3.653	207	42.842	3.625
105	41.337	4.747	208	43.104	4.454
106	41.028	4.404	209	43.124	4.075
108	40.916	3.194	210	41.366	3.780
109	41.146	3.400	212	42.986	3.794
111	41.131	3.077	213	43.163	4.284
112	41.239	2.716	214	42.557	3.266
113	40.822	2.623	215	43.226	3.502
114	41.064	2.716	219	41.539	2.901
115	40.980	2.361	220	42.468	2.883
116	41.361	2.909	221	41.376	2.924
117	40.698	2.404	222	42.292	3.393
118	41.143	4.853	223	42.831	3.643
119	41.020	2.702	228	42.581	4.730
121	41.003	2.942	230	42.579	3.656
122	41.278	3.073	231	42.252	3.605
123	40.672	2.799	232	41.961	3.719
124	41.001	3.200	233	44.042	5.681
200	40.861	4.761	234	43.96	5.239
201	41.831	3.406	**Sum**	**1840.791**	**158.013**
202	42.033	3.718	**Mean**	**41.836**	**3.591**
			STD	**0.942**	**0.771**

Table 7. The study evaluation time comparison in personal computer (PC) and smartphone for the MIT-BIH Arrhythmia database. (N/A = not available).

Study	Arrhythmia	Device Evaluation Time (S)	
		Smartphone	PC
Proposed study	Normal, APC, VPC, AF, VF	1840.791	158.013
Chakroborty et al. [48]	Normal, APC, VPC, LBBB, RBBB	N/A	6875.3

5. Conclusions

This study has developed an integrated method from several algorithms for arrhythmia detection by applying the relatively less complicated algorithms, which has purposed of the real-time wearable device for the arrhythmia detection. The system performs based on the R-R interval and the raw ECG signal for detecting the ECG abnormalities. This study evaluated 169 records from four databases in PhysioNet. Our study results for SVEB (i.e., APC) and VEB (i.e., VPC) have improved as compared to a previous study by utilizing the evaluation of ANSI/AAMI EC57:2012. For AF detection, most of the evaluations provide a positive achievement except for the episode sensitivity. Meanwhile, for VF, the episode sensitivity provides the decision from the whole databases ranging from 83% to 100%,

except for the MITDB episode positive predictivity, which is 75%. In conclusion, our integrated algorithm detection can achieve a good accuracy in comparison to other previous studies. However, more advanced algorithms, faster MCU & BLE devices, and dry electrodes will be utilized as future works for our study. This will be a big advantage in solving data transfer problem and allow dry electrode multi-lead ECG system for more advanced arrhythmia detection and better evaluation.

Acknowledgments: This research is financially supported by Cal-Comp Electronics & Communications Co., Ltd., and Kinpo Electronics, Inc. New Taipei City, Taiwan. This research is also supported by Innovation Center for Big Data and Digital Convergence, Yuan Ze University, Taiwan.

Author Contributions: M.S., C.-H.L. and Y.-T.L. developed the algorithms and analyzed the data. Y.H. designed the Firmware. C.-C.K. designed the hardware. M.S. wrote the paper. J.-S.S., M.F.A., J.C.C. and K.H. evaluated and supervised the study.

Conflicts of Interest: The authors declare no conflict of interest.

References

1. Shany, T.; Redmond, S.J.; Narayanan, M.R.; Lovell, N.H. Sensors-based wearable systems for monitoring of human movement and falls. *IEEE Sens. J.* **2012**, *12*, 658–670. [CrossRef]
2. Patel, S.; Lorincz, K.; Hughes, R.; Huggins, N.; Growdon, J.; Standaert, D.; Akay, M.; Dy, J.; Welsh, M.; Bonato, P. Monitoring motor fluctuations in patients with Parkinson's disease using wearable sensors. *IEEE Trans. Inf. Technol. Biomed.* **2009**, *13*, 864–873. [CrossRef] [PubMed]
3. Corbishley, P.; Rodríguez-Villegas, E. Breathing detection: Towards a miniaturized, wearable, battery-operated monitoring system. *IEEE Trans. Biomed. Eng.* **2008**, *55*, 196–204. [CrossRef] [PubMed]
4. Guo, H.W.; Huang, Y.S.; Chien, J.C.; Shieh, J.S. Short-term analysis of heart rate variability for emotion recognition via a wearable ECG device. In Proceedings of the IEEE International Conference on Intelligent Informatics and Biomedical Sciences (ICIIBMS), Okinawa, Japan, 28–30 November 2015; pp. 262–265.
5. Rosenberg, M.A.; Samuel, M.; Thosani, A.; Zimetbaum, P.J. Use of a noninvasive continuous monitoring device in the management of atrial fibrillation: A pilot study. *Pacing Clin. Electrophysiol.* **2013**, *36*, 328–333. [CrossRef] [PubMed]
6. Baig, M.M.; Gholamhosseini, H.; Connolly, M.J. A comprehensive survey of wearable and wireless ECG monitoring systems for older adults. *Med. Biol. Eng. Comput.* **2013**, *51*, 485–495. [CrossRef] [PubMed]
7. Fensli, R.; Gunnarson, E.; Gundersen, T. A wearable ECG-recording system for continuous arrhythmia monitoring in a wireless tele-home-care situation. In Proceedings of the 18th IEEE Symposium on Computer-Based Medical Systems, Dublin, Ireland, 23–24 June 2005; pp. 407–412.
8. Lin, C.T.; Chang, K.C.; Lin, C.L.; Chiang, C.C.; Lu, S.W.; Chang, S.S.; Lin, B.S.; Liang, H.Y.; Chen, R.J.; Lee, Y.T.; et al. An intelligent telecardiology system using a wearable and wireless ECG to detect atrial fibrillation. *IEEE Trans. Inf. Technol. Biomed.* **2010**, *14*, 726–733. [PubMed]
9. Hu, S.; Wei, H.; Chen, Y.; Tan, J. A real-time cardiac arrhythmia classification system with wearable sensor networks. *Sensors* **2012**, *12*, 12844–12869. [CrossRef] [PubMed]
10. Hadiyoso, S.; Usman, K.; Rizal, A. Arrhythmia detection based on ECG signal using Android mobile for athlete and patient. In Proceedings of the IEEE 3rd International Conference on Information and Communication Technology (ICoICT), Nusa Dua, Bali, 27–29 May 2015; pp. 166–171.
11. Fuster, V.; Rydén, L.E.; Cannom, D.S.; Crijns, H.J.; Curtis, A.B.; Ellenbogen, K.A.; Halperin, J.L.; Le Heuzey, J.Y.; Kay, G.N.; Lowe, J.E.; et al. ACC/AHA/ESC 2006 guidelines for the management of patients with atrial fibrillation–executive summary: A report of the American College of Cardiology/American Heart Association Task Force on practice guidelines and the European Society of Cardiology Committee for Practice Guidelines (Writing Committee to Revise the 2001 Guidelines for the Management of Patients with Atrial Fibrillation) Developed in collaboration with the European Heart Rhythm Association and the Heart Rhythm Society. *Eur. Heart J.* **2006**, *27*, 1979–2030. [PubMed]
12. Wolf, P.A.; Abbott, R.D.; Kannel, W.B. Atrial fibrillation as an independent risk factor for stroke: The Framingham Study. *Stroke* **1991**, *22*, 983–988. [CrossRef] [PubMed]
13. Kara, S.; Okandan, M. Atrial fibrillation classification with artificial neural networks. *Pattern Recognit.* **2007**, *40*, 2967–2973. [CrossRef]

14. Roonizi, E.K.; Sassi, R. Dominant atrial fibrillatory frequency estimation using an extended Kalman smoother. In Proceedings of the Computing in Cardiology Conference (CinC), Vancouver, BC, Canada, 11–14 September 2016; pp. 989–992.
15. Mohebbi, M.; Ghassemian, H. Detection of atrial fibrillation episodes using SVM. In Proceedings of the EMBS 30th Annual International Conference of the IEEE Engineering in Medicine and Biology Society, Vancouver, BC, Canada, 20–25 August 2008; pp. 177–180.
16. Abdul-Kadir, N.A.; Safri, N.M.; Othman, M.A. Dynamic ECG features for atrial fibrillation recognition. *Comput. Methods Progr. Biomed.* **2016**, *136*, 143–150. [CrossRef] [PubMed]
17. Rajpurkar, P.; Hannun, A.Y.; Haghpanahi, M.; Bourn, C.; Ng, A.Y. Cardiologist-Level Arrhythmia Detection with Convolutional Neural Networks. *arXiv* **2017**, arXiv:1707.01836.
18. McWilliam, J.A. Cardiac failure and sudden death. *Br. Med. J.* **1889**, *1*, 6. [CrossRef] [PubMed]
19. Weaver, W.D.; Copass, M.K.; Bufi, D.; Ray, R.; Hallstrom, A.P.; Cobb, L.A. Improved neurologic recovery and survival after early defibrillation. *Circulation* **1984**, *69*, 943–948. [CrossRef] [PubMed]
20. Alonso-Atienza, F.; Rojo-Álvarez, J.L.; Rosado-Muñoz, A.; Vinagre, J.J.; García-Alberola, A.; Camps-Valls, G. Feature selection using support vector machines and bootstrap methods for ventricular fibrillation detection. *Expert Syst. Appl.* **2012**, *39*, 1956–1967. [CrossRef]
21. Anas, E.M.A.; Lee, S.Y.; Hasan, M.K. Exploiting correlation of ECG with certain EMD functions for discrimination of ventricular fibrillation. *Comput. Biol. Med.* **2011**, *41*, 110–114. [CrossRef] [PubMed]
22. Thong, T.; McNames, J.; Aboy, M.; Goldstein, B. Prediction of paroxysmal atrial fibrillation by analysis of atrial premature complexes. *IEEE Trans. Biomed. Eng.* **2004**, *51*, 561–569. [CrossRef] [PubMed]
23. Sayadi, O.; Shamsollahi, M.B.; Clifford, G.D. Robust detection of premature ventricular contractions using a wave-based Bayesian framework. *IEEE Trans. Biomed. Eng.* **2010**, *57*, 353–362. [CrossRef] [PubMed]
24. Özbay, Y.; Ceylan, R.; Karlik, B. A fuzzy clustering neural network architecture for classification of ECG arrhythmias. *Comput. Biol. Med.* **2006**, *36*, 376–388. [CrossRef] [PubMed]
25. Song, M.H.; Lee, J.; Cho, S.P.; Lee, K.J.; Yoo, S.K. Support vector machine based arrhythmia classification using reduced features. *Int. J. Control Autom. Syst.* **2005**, *3*, 571.
26. Zhou, X.; Ding, H.; Wu, W.; Zhang, Y. A real-time atrial fibrillation detection algorithm based on the instantaneous state of heart rate. *PLoS ONE* **2015**, *10*, e0136544. [CrossRef] [PubMed]
27. Gowid, S.; Dixon, R.; Ghani, S. Performance Comparison Between Fast Fourier Transform-Based Segmentation, Feature Selection, and Fault Identification Algorithm and Neural Network for the Condition Monitoring of Centrifugal Equipment. *J. Dyn. Syst. Meas. Control* **2017**, *139*, 061013. [CrossRef]
28. Bucci, O.M.; Migliore, M.D. A Novel Nonuniform Fast Fourier Transform Algorithm and Its Application to Aperiodic Arrays. *IEEE Antennas Wirel. Propag. Lett.* **2017**, *16*, 1472–1475. [CrossRef]
29. Glowacz, A. Recognition of Acoustic Signals of Loaded Synchronous Motor Using FFT, MSAF-5 and LSVM. *Arch. Acoust.* **2015**, *40*, 197–203. [CrossRef]
30. Kotus, J. Multiple sound sources localization in free field using acoustic vector sensor. *Multimedia Tools Appl.* **2015**, *74*, 4235–4251. [CrossRef] [PubMed]
31. Clayton, R.H.; Murray, A. Estimation of the ECG signal spectrum during ventricular fibrillation using the fast Fourier transform and maximum entropy methods. In Proceedings of the IEEE Computers in Cardiology, London, UK, 5–8 September 1993; pp. 867–870.
32. Afonso, V.X.; Tompkins, W.J. Detecting ventricular fibrillation. *IEEE Eng. Med. Biol. Mag.* **1995**, *14*, 152–159. [CrossRef]
33. Analog Devices. Single-Lead, Heart Rate Monitor Front End. AD8232 Datasheet. 2012. Available online: http://www.analog.com/media/en/technical-documentation/data-sheets/AD8232.pdf (accessed on 30 September 2017).
34. Goldberger, A.L.; Amaral, L.A.; Glass, L.; Hausdorff, J.M.; Ivanov, P.C.; Mark, R.G.; Mietus, J.E.; Moody, G.B.; Peng, C.K.; Stanley, H.E. Physiobank, physiotoolkit, and physionet. *Circulation* **2000**, *101*, e215–e220. [CrossRef] [PubMed]
35. Nolle, F.M.; Badura, F.K.; Catlett, J.M.; Bowser, R.W.; Sketch, M.H. CREI-GARD, a new concept in computerized arrhythmia monitoring systems. *Comput. Cardiol.* **1986**, *13*, 515–518.
36. Moody, G.B.; Mark, R.G. The impact of the MIT-BIH arrhythmia database. *IEEE Eng. Med. Biol. Mag.* **2001**, *20*, 45–50. [CrossRef] [PubMed]

37. Moody, G.B.; Muldrow, W.; Mark, R.G. A noise stress test for arrhythmia detectors. *Comput. Cardiol.* **1984**, *11*, 381–384.
38. Association for the Advancement of Medical Instrumentation. *Testing and Reporting Performance Results of Cardiac Rhythm and st Segment Measurement Algorithms*; ANSI/AAMI EC57; Association for the Advancement of Medical Instrumentation: Arlington, VA, USA, 2012.
39. Hamilton, P.S.; Tompkins, W.J. Quantitative investigation of QRS detection rules using the MIT/BIH arrhythmia database. *IEEE Trans. Biomed. Eng.* **1986**, *12*, 1157–1165. [CrossRef]
40. Hamilton, P.S. *Open Source ECG Analysis Software Documentation*; EP Limited: Somerville, MA, USA, 2002.
41. Richman, J.S.; Moorman, J.R. Physiological time-series analysis using approximate entropy and sample entropy. *Am. J. Physiol. Heart Circ. Physiol.* **2000**, *278*, H2039–H2049. [PubMed]
42. Lin, C.H.; Chien, J.C.; Haraikawa, K.; Huang, Y.S.; Guo, H.W.; Shieh, J.S. A modular integrating algorithm for multiple arrhythmia detection. In Proceedings of the IEEE International Conference on Communication Problem-Solving (ICCP), Taipei, Taiwan, 7–9 September 2016; pp. 1–2.
43. Lo, M.T.; Lin, L.Y.; Hsieh, W.H.; Ko, P.C.I.; Liu, Y.B.; Lin, C.; Chang, Y.C.; Wang, C.Y.; Young, V.H.W.; Chiang, W.C.; et al. A new method to estimate the amplitude spectrum analysis of ventricular fibrillation during cardiopulmonary resuscitation. *Resuscitation* **2013**, *84*, 1505–1511. [CrossRef] [PubMed]
44. De Chazal, P.; O'Dwyer, M.; Reilly, R.B. Automatic classification of heartbeats using ECG morphology and heartbeat interval features. *IEEE Trans. Biomed. Eng.* **2004**, *51*, 1196–1206. [CrossRef] [PubMed]
45. Young, B.; Brodnick, D.; Spaulding, R. A comparative study of a hidden Markov model detector for atrial fibrillation. In Proceedings of the IEEE Signal Processing Society Workshop Neural Networks for Signal Processing IX, Madison, WI, USA, 23–25 August 1999; pp. 468–476.
46. Park, S.B.; Yoon, H.R. Development and Evaluation of an Improved Algorithm for Detection of Ventricular Fibrillation. In *World Congress on Medical Physics and Biomedical Engineering 2006*; Springer: Berlin/Heidelberg, Germany, 2007; pp. 1174–1177.
47. Moraes, J.C.T.B.; Blechner, M.; Vilani, F.N.; Costa, E.V. Ventricular fibrillation detection using a leakage/complexity measure method. In Proceedings of the IEEE Computers in Cardiology, Memphis, TN, USA, 22–25 September 2002; pp. 213–216.
48. Chakroborty, S.; Patil, M.A. Real-time arrhythmia classification for large databases. In Proceedings of the 36th Annual International Conference of the IEEE Engineering in Medicine and Biology Society (EMBC), Chicago, IL, USA, 26–30 August 2014; pp. 1448–1451.
49. Logan, B.; Healey, J. Robust detection of atrial fibrillation for a long term telemonitoring system. In Proceedings of the IEEE Computers in Cardiology, Lyon, France, 25–28 September 2005; pp. 619–622.
50. Hoffmann, K.P.; Ruff, R. Flexible dry surface-electrodes for ECG long-term monitoring. In Proceedings of the 29th Annual International Conference of the IEEE Engineering in Medicine and Biology Society, Lyon, France, 22–26 August 2007; pp. 5739–5742.
51. Abdoli-Eramaki, M.; Damecour, C.; Christenson, J.; Stevenson, J. The effect of perspiration on the sEMG amplitude and power spectrum. *J. Electromyogr. Kinesiol.* **2012**, *22*, 908–913. [CrossRef] [PubMed]
52. Baba, A.; Burke, M.J. Measurement of the electrical properties of ungelled ECG electrodes. *Int. J. Biol. Biomed. Eng.* **2008**, *2*, 89–97.
53. Gargiulo, G.D.; Bifulco, P.; Cesarelli, M.; Fratini, A.; Romano, M. Problems in assessment of novel biopotential front-end with dry electrode: A brief review. *Machines* **2014**, *2*, 87–98. [CrossRef]
54. Winter, B.B.; Webster, J.G. Reductionl of interference due to common mode voltage in biopotential amplifiers. *IEEE Trans. Biomed. Eng.* **1983**, *1*, 58–62. [CrossRef]
55. Chi, Y.M.; Jung, T.P.; Cauwenberghs, G. Dry-contact and noncontact biopotential electrodes: Methodological review. *IEEE Rev. Biomed. Eng.* **2010**, *3*, 106–119. [CrossRef] [PubMed]

2.

Predicting the Percentage of Atrial Fibrillation using Sample Entropy

Predicting the Percentage of Atrial Fibrillation using Sample Entropy

Muammar Sadrawi, Bhekumuzi Mathunjwa,
Jiann-Shing Shieh
Dept. Mechanical Engineering and Innovation Center for
Big Data and Digital Convergence Yuan Ze University.
Chung-Li, Taiwan

Koichi Haraikawa, Jen Chien Chien
Health and Beauty Research Center
Kinpo Electronics, Inc.
New Taipei City, Taiwan

Han Wen Guo
Health and Beauty Research Center
Cal-Comp Inc.
New Taipei City, Taiwan

Maysam F. Abbod
Dept. Electronic and Computer Engineering
Brunel University London
Uxbridge, UK

***Abstract*- Atrial fibrillation is the most commonly confronted cardiac arrhythmia in humans. This paper is written to use sample entropy and percentage of atrial fibrillation as a measure of regularity to measure AF. To assume the percentage of AF, 25 long-term ECG recordings of human subjects with atrial fibrillation containing a total of 299 AF episodes were processed. The mean and SD of percentage breaking point in all the subjects from the MIT-BIH Atrial Fibrillation database was 0.606±0.086, and its sample entropy is 0.352±0.151. The mean and SD for sample entropy at 100% AF is 1.067±0.452. This data is used to predict the percentage of AF at a given sample entropy value. Our study concludes that the early detection of AF can be initiated by the AF already happened for 60%.**

I. INTRODUCTION

According to a study, atrial fibrillation is an irregular supraventricular tachyarrhythmia dealing with the degradation of the atrial system [1]. Atrial fibrillation (AF) is the most frequently happened arrhythmia. It affects about 5% of the adult population and around 10% of the population over 60 years of age [2-3]. It is the most commonly known cardiac cause of stroke [4]. Due to its relation with high risk for heart failure, stroke and sudden deaths, AF has a high influence on the longevity and quality of life of a number of people [5-6]. During atrial fibrillation, most symptoms are irregular ventricular rate, and associated risk of death is common in patients with history of atrial fibrillation [7-8].

Heart rate variability (HRV) analysis for the AF cases have been evaluated by previous studies. The shortened HRV was discovered in for the AF cases [9]. The study related to the increased HRV regularity for the AF cases has been evaluated [10]. The optimization for the sample entropy parameters related to the AF cases has been conducted by Alcaraz et al., [11]. This study has the purpose for the early detection of the AF by evaluating the corresponding heart rate regularity by utilizing the sample entropy to the AF percentage.

II. MATERIAL AND METHODOLOGY

A. Materials

ECG data for this study were obtained from MIT-BIH Atrial Fibrillation database to find the percentage of AF with sample entropy. The database contains 25 long term ECG recordings of human subjects with AF containing a total of 299 AF episodes. The individual recordings are each 10 hours in duration, and contain two ECG signals each sampled at 250 samples per seconds with 12-bit resolution over a range of ±10 millivolts. We used signals from lead II ECG only for our research which is the signal with most R-R peaks facing upwards.

B. Methodology

In this study, we utilize the sample entropy, as the useful measurement regularity. The entropy calculation was initially by the approximate entropy by Pincus et al., [12]. The modified approximate entropy, sample entropy, considering no self-matches, developed by Richman et al., [13]. Initially, the data set is specified by using the MIT-BIH Atrial Fibrillation database [14]. The annotation of the normal sinus rhythm followed by the AF is investigated. This specific phenomenon is trimmed to a condition of one minute before AF to a minute of full of the AF rhythm. By having this new reconstructed signal, the R-R interval is evaluated and sampled to 4 Hz. The calculation of the sample entropy is applied to evaluate the regularity of the heart rate. In this study, one minute sliding window is utilized for the sample entropy calculation. The breaking point from the normal sinus rhythm to the AF rhythm is evaluated by the rapid slope change. Figure 1 shows the detail flowchart of the study.

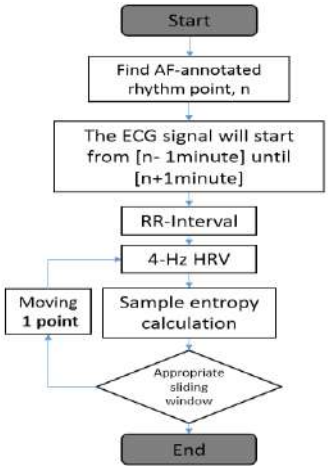

Figure 1. The flowchart of the percentage of atrial fibrillation detection.

III. RESULTS

This study evaluates the utilization of sample entropy for the whole normal sinus rhythm followed by the AF rhythm into a 2-minute segment. The results are evaluated based on the sample entropy of AF at breaking point and the sample entropy at 100% of AF, which can be seen by Fig. 2.

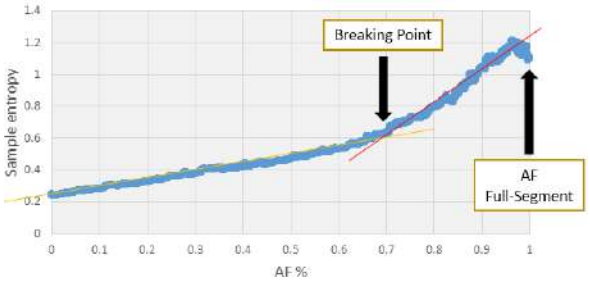

Figure 2. A subject correlating the percentage atrial fibrillation and the corresponding sample entropy.

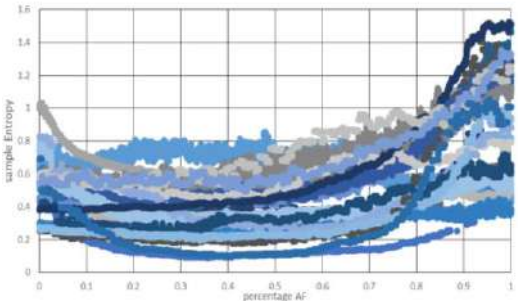

Figure 3. The whole subjects percentage atrial fibrillation and the corresponding sample entropy.

The whole case results can be seen by the figure 3. Each color represents each case. The evaluation produces the breaking point of the all subject is 0.606±0.086, and its sample entropy is 0.352±0.151 for the mean and the standard deviation. Furthermore, the 100% of atrial fibrillation signal will produce 1.067±0.452 of the sample entropy.

.

IV. CONCLUSION

This study evaluates the database of MIT-BIH Atrial Fibrillation containing the 25 ECG signals with 299 episodes totally. The results can be concluded that the possibility of the early detection of the AF can be recognized while the AF already happened for at least 60%.

The limitation of this study is by manually choosing the breaking point. For our future works, the decision to detect the breaking point should be developed by implementing either a simple or a complex algorithm.

REFERENCES

[1] V. Fuster, L.E. Rydén, R.W. Asinger, D.S. Cannom, H.J. Crijns, R.L. Frye, J.L. Halperin, G. Neal Kay, W.W. Klein, S. Levy, and R.L. McNamara, "ACC/AHA/ESC guidelines for the management of patients with atrial fibrillation," *European Heart Journal*, vol. 22, pp.1852-1923, 2001.

[2] S. Levy, G. Breithardt, R.W. Campbell, A.J. Camm, J.C. Daubert, M. Allessie, et al., "Atrial fibrillation: current knowledge and recommendations for management. Working Group on Arrhythmias of the European Society of Cardiology," *Eur Heart J*, vol. 19, pp. 1294-1320, 1998.

[3] E.J. Benjamin, D. Levy, S.M. Vaziri, R.B. D'Agostino, A.J. Belanger, and P.A. Wolf, "Independent risk factors for atrial fibrillation in a population-based cohort. The Framingham Heart Study," *JAMA*, vol. 271, pp. 840-844, 1994.

[4] P.A. Wolf, R.D. Abbot, W.B. and Kannel, "Atrial fibrillation as an independent risk factor for stroke: the Framingham Study," *Stroke*, vol. 22, pp. 983-988, 1991.

[5] I. Hajjar, and T.A. Kotchen, "Trends in prevalence, awareness, treatment, and control of hypertension in the United States, 1988-2000," *JAMA*, vol. 290, no. 2, pp. 199-206, 2003.

[6] T.S. Tsang, G.W. Petty, M.E. Barnes *et al.*, "The prevalence of atrial fibrillation in incident stroke cases and matched population controls in Rochester, Minnesota: changes over three decades," *J Am Coll Cordial*, vol. 42, no. 1, pp. 93-100, 2003.

[7] A.D. Krahn, J. Manfreda, R.B. Tate, F.A. Mathewson, T.E. Cuddy, "The natural history of atrial fibrillation: incidence, risk factors, and prognosis in the Manitoba Follow-Up Study," *Am J Med*, vol. 98, pp. 476-484, 1995.

[8] S. Stewart, K. Maclntyre, J.W. Chalmers, et. al, "Trends in case-fatality in 22968 patients admitted for the first time with atrial fibrillation in Scotland," *Int. J. Cardiol*., vol. 82, pp. 229-236, 2002.

[9] M. Sosnowski, P. W. Macfarlane, & M. Tendera, "Determinants of a reduced heart rate variability in chronic atrial fibrillation," *Annals of Noninvasive Electrocardiology*, vol. 16, pp. 321-326, 2011.

[10] R. Sungnoon, S. Muengtaweepongsa, P. Kitipawong, K. Suwanprasert, and T. Ngarmukos, "Increased sample entropy in atrial fibrillation relates to cardiac autonomic dysfunction determined by heart rate variability: A preliminary study," *Biomedical Engineering International Conference (BMEiCON)*, pp. 1-4, 2012.

[11] R. Alcaraz, D. Abásolo, R. Hornero and J.J. Rieta," Optimal parameters study for sample entropy-based atrial fibrillation organization analysis," *computer methods and programs in biomedicine*, vol. 99, pp.124-132, 2010.

[12] S.M. Pincus, I.M. Gladstone, and R.A. Ehrenkranz, "A regularity statistic for medical data analysis," *Journal of clinical monitoring*, vol. 7, pp.335-345, 1991.

[13] J.S. Richman and J.R. Moorman, "Physiological time-series analysis using approximate entropy and sample entropy," *American Journal of Physiology-Heart and Circulatory Physiology*, vol. 278, pp. H2039-H2049, 2000.

[14] A.L. Goldberger, L.A. Amaral, L. Glass, J.M. Hausdorff, P.C. Ivanov, R.G. Mark, J.E. Mietus, G.B. Moody, C.K. Peng and H.E. Stanley, "Physiobank, physiotoolkit, and physionet components of a new research resource for complex physiologic signals," *Circulation*, vol. 101, pp. e215-e220. 2000.

3.

A Modular Integrating Algorithm for Multiple Arrhythmia Detection

A Modular Integrating Algorithm for Multiple Arrhythmia Detection

Chien-Hung Lin[1], Jen-Chien Chien[1], Koichi Haraikawa[1], Yu-Shun Huang[1], Han-Wen Guo[1], and Jiann-Shing Shieh[2]

[1]Health and Beauty Research Center, Kinpo Electronics, Inc.
New Taipei City, Taiwan
[2]Mechanical Engineering Department, Yuan Ze University
Chung-Li, Taiwan

***Abstract*—The purpose of this paper is to propose a modular integrating algorithm. This algorithm can let the program detect multiple arrhythmias and is very easy to add more diseases detection algorithm. Also, it can save the repeated calculations in multiple algorithms. By a real test of the program, the result is that the computing time of the integrating algorithm is 46.86% less than the sum of the computing time of all individual algorithms. And the average accuracy is also improved from 94.73% to 95.35%.**

Keywords—Arrhythmia detection, ECG processing, Integrating algorithm

I. INTRODUCTION

Many current relative researches of ECG are to use the program to automatically diagnose arrhythmia and the different arrhythmias have their algorithms to automatically detect. But clinically the detection of single arrhythmia is not enough. There are usually several arrhythmias have to be mainly and necessarily detected. So an algorithm that can be flexibly increased the detectable arrhythmia is worthy of a developing goal.

The general method is first using "morphological" or "dynamic" concept to get features and then distinguish different arrhythmias by using the classifier "SVM" or "Artificial Neural Network". In these kinds of methods, extracting features is usually a part that needs huge calculation. Besides, the training of the classifier and the choosing of the training data are also relative with the kinds and numbers of the target arrhythmia. Acharya et al [1] uses spectral entropy, Poincare plot geometry and largest Lyapunov exponent (LLE) of RR interval, then uses artificial neural networks (ANNs) to classify them. Asl et al [2] uses fifteen features which are further extracted from HRV and then uses generalized discriminant analysis (GDA) to reduce the dimensions of features. And then finally use support vector machine (SVM) to classify them. The fifteen features in this method include time domain features, frequency domain features, and nonlinear parameters. In nonlinear parameters, except spectral entropy, LLE which are like [1], there are still approximate entropy and detrended fluctuation analysis (DFA). Ye et al [3] uses morphological and dynamic features at the same time and then uses SVM to classify them. Morphological features use wavelet transform and independent component analysis. And dynamic feature also uses RRI. Oresko et al [4] uses the method "waveform comparison" and some general features (RRI, QRS width, beat width) and then uses feedforward multilayer perceptron (MLP) artificial neural network (ANN) to determine arrhythmia. Gradl et al [5] first uses the method "Template comparing" to deal with ECG and then extracts features which are difference in absolute area (ArDiff), maximal cross-correlation coefficient (MaxCorr), RRI, QRS width,…etc., then classify them by a decision tree.

We find that the above-mentioned methods are mostly to use the features based on RRI or HRV. But some features are more suitable to find some arrhythmias and the classifiers are needed to be trained. If the new target arrhythmia needs to be added, choosing data, training and adjusting are needed to be done again. So we propose a modular integrating detection method to let the accuracy of detections keep the same level and integrate classified problems at the same time. We summarize the features which are needed by integrated algorithms. First, find out R peak and then individually identify QRS complex, T wave, P wave. With these basic feature data, we can soon integrate PVC detection via Iliev et al. method [6] and the detection of PAC and 1 degree AV block which are developed by us.

II. METHODS

A. Filtering and R peak detection

Filtering and R peak detection are always the first step for extracting features. We use a band-pass finite impulse response (FIR) filter to remove noise. And then by referring to the method of Iliev et al [6], we use three dynamic thresholds to check the change of the slope for finding R peak.

B. QRS determining and T detection

We base on the features of the waveform of QRS complex wave and T wave to design a logical flowchart for detection. We use the mean-shifted first-order derivative of ECG to find the points that their derivative changes sign. These points are candidates of peak. By the mean and standard deviation of derivative of these peaks, we decide upper and lower thresholds. When derivative of a peak exceeds the threshold, this peak is an R peak. And the sign of derivative determines the polarity of the QRS complex. According to the wave characteristics of the QRS complex and a fixed window, we can find out Q and R from candidates of peak and find onset

and offset of this QRS complex. The T wave detection is by deciding a window size according to RRI. Then similar the QRS processing, we pick the candidates of peak and find out onset, peak and offset of T.

C. P detection

Because the amplitude of P wave is possibly small and easy to be confused with noise, we first use the band-pass filter to filter the signal. Then determine the search window according to RRI and find peaks. Peaks number and sign can decide the polarity and position of P wave. Then, we find the point which is the most changing of the slope round P to be onset and offset. About the Gibbs ring effect occurred after filtering, our method is similar with Oresko et al [4]. We use the position and voltage as the reference and choose a point that can let P wave be closed to a full waveform in the filtered signal for solving the "unfound offset" condition. For the possible condition of "no P wave", we delete improper P wave according to its ratio of length to width.

D. Arrhythmia detection

As the purpose of this paper, we use three algorithms to detect three arrhythmias. PVC detection mainly refers to the feature extraction method of QRS pattern waveform of Iliev et al [6]. By the changing degree of RRI and waveform similarity estimated by a sampled array, we can classify normal beats and PVC. With the data of P wave and QRS complex detected by the aforementioned algorithm, 1 degree AV block is detected when the related distance between P wave and QRS complex is out of some thresholds. PAC detection uses several information of PQRST, including P wave width, P wave height, PR interval, RR interval, QRS complex width…etc. A trained ANN classifier can use these data to determine the PAC beats.

III. IMPLEMENTATION

We use the 46 records in the MIT-BIH Arrhythmias Database. For simulating the one lead device that we want to use, we choose the Lead II signal in this database. Therefore two records, 102 and 104, which do not include Lead II signal does not be used. In order to correspond with the data processing mode which is dealing with five minutes ECG data at one time, we only use the data of thirty minutes for each record. In program implementation, we let each detection stage to be an independent algorithm object and design a data objects to store the results of algorithm objects. (Figure 1) According to this program flowchart, comparing results about the calculation time and the accuracy can be obtained.

IV. RESULTS AND DISCUSSIONS

After testing, we get the improvement rate of computing time is 46.86% (time spend by integrated method is 96.52sec, 181.62sec by normal method). The accuracy is slightly better because some false case is fixed by other detection.

The orientation of the research in the future can be to increase the detecting modules for other arrhythmias or to let the program be easy to build in the mobile platform by trying to divide the computing of all flow into several stages.

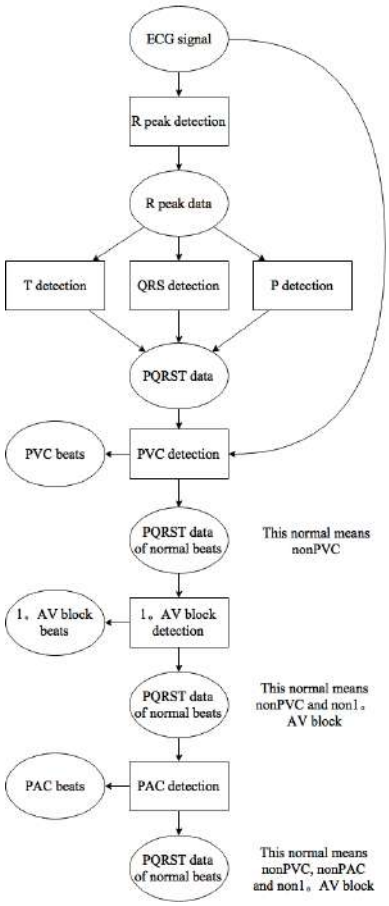

Figure 1. Flowchart of several independent algorithm and data objects

ACKNOWLEDGMENT

This research was financially supported by Cal-Comp, and Kinpo Electronics, Inc. New Taipei City, Taiwan.

REFERENCES

[1] R. Acharya, A. Kumar, P.S. Bhat, C.M. Lim, S.S. lyengar, N. Kannathal, S.M. Krishnan, "Classification of cardiac abnormalities using heart rate signals," *Med. Biol. Eng. Comput*., 2004, 42, 288-293.

[2] B. M. Asl, S. K. Setarehdan, M. Mohebbi, "Support vector machine-based arrhythmia classification using reduced features of heart rate variability signal," *Artificial Intelligence in Medicine* (2008) 44, 51—64.

[3] C. Ye, M.T. Coimbra, B.V.K. V.Kumar, "Arrhythmia Detection and Classification using Morphological and Dynamic Features of ECG Signals," *Annual International Conference of the IEEE EMBS* Buenos Aires, Argentina, August 31 - September 4, 2010.

[4] J.J. Oresko and Z. Jin, J. Cheng, S. Huang, Y. Sun, H. Duschl, and A.C. Cheng, "A Wearable Smartphone-Based Platform for Real-Time Cardiovascular Disease Detection Via Electrocardiogram Processing," *IEEE TRANSACTIONS ON INFORMATION TECHNOLOGY IN BIOMEDICINE*, VOL. 14, NO. 3, MAY 2010.

[5] S. Gradl, P. Kugler, C. Lohm¨uller, B. Eskofier, "Real-time ECG monitoring and arrhythmia detection using Android-based mobile devices," in 34th *Annual International Conference of the IEEE EMBS* San Diego, California USA, 28 August - 1 September, 2012.

[6] I. Iliev, V. Krasteva, S. Tabakov, "Real-time detection of pathological cardiac events in the electrocardiogram," *Physiol. Meas*. 28 (2007) 259–276.

4.

A Threshold-based Algorihum of Fall Detection Using a Wearable Device with Tri-axial Accelerometer and Gyroscope

A Threshold-based Algorihum of Fall Detection Using a Wearable Device with Tri-axial Accelerometer and Gyroscope

Han Wen Guo
Yu Shun Huang
Yi Ta Hsieh
Healthcare & Beauty Research Center
Cal-comp Inc., New Taipei City, Taiwan

Jen Chien Chien
Koichi Haraikawa
Healthcare & Beauty Research Center
Kinpo Inc., New Taipei City, Taiwan

Jiann Shing Shieh
Department of Mechanical Engineering,
Yuan Ze University, Taoyuan, Taiwan

***Abstract*—Fall events are the external causes of injury in the elderly adults, even leading to disability and death. In this study, we used a weightless and wearable device with built-in tri-axial accelerometer and gyroscope to record 8 types of stimulated-falls and 6 types of different ADL preformed by 6 health young subjects. A threshold-based algorithm using our device was developed to determine a fall event. Using our fall detection system, falls could be distinguished from ADL successfully for a total data set.**

Keywords—fall detection; accelerometer; gyroscopes; wearable system

I. INTRODUCTION

Fall events are the external causes of injury in the elderly adults. According the WHO report, approximately 28-35% of people aged of 65 and over fall each year increasing to 32-42% for those over 70 years of age [1]. Fall events cause not only severe injury but also disability for elderly adults. In 2000, the relative financial costs of fall event were estimated to be approximately $20 billion and increase to $54.9 billion by 2020 [2]. An emergency response system has been developed to facilitate calling for help after a fall event. However, in some severe case of emergency cases, the emergency response system may not be able to active [3, 4]. Hence, reliable and automatic fall detection became more important for aging society.

In recent years, numerous approaches by using portable sensors were developed for the automatic detection of falls. Many stragies utilized the change in aceleration magnitude to determine falls. However, focusing on large acceleration result only in many false positiving as other activities such as sitting and running. [5, 6] Other fall detections rely on detection of body orientation after a fall. These methods may be affected by activities with similar posture and are less effective when the falling posture is not horizontal.

Using both accelerometer and gyroscope sensor for the fall detection was demostrated in the previous studies [7, 8]. When fall event occuring, the accelerometer provides valuable information of body inertial change due to the impact. Simultaneously, the gyroscope provides the unique information of body's rotational velocity during a fall event. A fall event produces both large change of acceleration and angular velocity. These changes are not observed during normal daily activities [8]. Thus, several thresholds of acceleration and angular velocity were set to distinigh between fall event and ADL.

In this study, we developed a weightless and wearable device with built-in tri-axial accelerometer and gyroscope to record 8 types of stimulated-falls and 6 types of different ADL preformed by 6 health young subjects. A threshold-based algorithm using our device was developed to determine a fall event. The feasibility of our fall detection system was demonstrated in this work.

II. MATERIALS AND METHOD

A. Wearable system and data acquisition

A wearable system (XYZlife BC1, Kinpo Inc, Taipei, Taiwan) is composed of a fitting clothing and a wearable device BC1 with built-in tri-axial accelerometer and gyroscope (MPU-6500, InvenSense Inc., San Jose, US) which were used for data acquisition. The sensor signals were recorded at a frequency of 1k Hz and resolution of 16 bits, and saved in a tablet PC via a Bluetooth module.

During recording, subject wears a fitting clothing with BC1 device, which is placed in front of right chest as shown in Fig. 1.

B. The simulated fall and ADL study

The simulated fall study involved 6 young healthy (<40 years) subjects. The subjects ranged in age from 30 to 39 years (35.2±2.2 years), body mass from 59 to 76 kg (75.2±2.2 kg), and height from 1.68 to 1.76 m (1.75±0.2 m) have been recruited for this study. Subjects performed eight different types of simulated-falls onto large crash mats under supervision condition. Tri-axial accelerometer and gyroscope signal were recorded during each simulated-falls via BC1 device.

Fig. 1. A fitting clothing with BC1 device, which is placed in front of right chest (red square). Built-in tri-axial accelerometer and gyroscope were used to collect the signal of acceleration and angular velocity.

Standing height occurred most commonly and caused injury to elderly people. Thus, falls from standing height in all directions should be stimulated [9]. Falls with knee flexion were also examined, similar to those observed in previous studies [10, 11]. The simulated-falls performed were: stand foreword fall (F fall), stand back fall (B fall), stand left lateral (SL fall), stand right lateral fall (SR fall), stand foreword fall with keen flexion (F fall_KF), stand back fall with keen flexion (B fall_KF), stand left lateral with keen flexion (SL fall_KF), and stand right lateral fall with keen flexion (SR fall_KF).

The second of this study involved the same subjects performing ADL after stimulated-falls. The ADL chosen were the actives that may cause the large change of acceleration and angular velocity and carried out during normal daily life for elderly adults. Thus, the activities performed as follows:

1. Waking 8 m.
2. Stooping down and touching the ground.
3. Sitting down and standing up from a chair (height, 45 cm).
4. Lying down and getting up from a bed (height, 15 cm).

C. The fall algorithm

The parameters used in analyses are similar to the previous studies [1,8]. The total sum acceleration vector, *Acc*, containing both static and dynamic acceleration componets, is caculated from sampled data using

$$Acc = \sqrt{(A_x)^2 + (A_y)^2 + (A_z)^2},$$

where A_x, A_y, and A_z are the accelerations (g) in the *x*, *y*, and *z* direstions. Also, angular velocity is calculated from sampled data as indicated in the following:

$$gyro = \sqrt{(\omega_x)^2 + (\omega_y)^2 + (\omega_z)^2},$$

Where ω_x, ω_y, and ω_z are angular velocities in *x*, *y*, and *z* directions.

When the subject falls, the acceleration is changing rapidly and the angular velocity is also increasing along fall direction. Critical threshold in the acceleration and angular velocity are used to determining a fall event. These critical thresholds are defined and derived as follows:

1. FT1 (lower acceleration fall threshold): local minima for the *Acc* signal of each recorded activity are referred to as the signal lower peak values (LPVs). The FT1 for the acceleration signals is set for the smallest upper fall peak recorded.
2. FT2 (upper acceleration fall threshold): local maxima for the *Acc* signal of each recorded activity are referred to as the signal upper peak values (UPVs). The FT2 for the acceleration signals is set for the largest upper fall peak recorded.
3. FT3 (lower angular velocity fall threshold): local maxima for the *gyro* signal of each recorded activity are referred to as the signal UPVs. The FT3 for the angular velocity signals is set for the largest upper fall peak recorded.

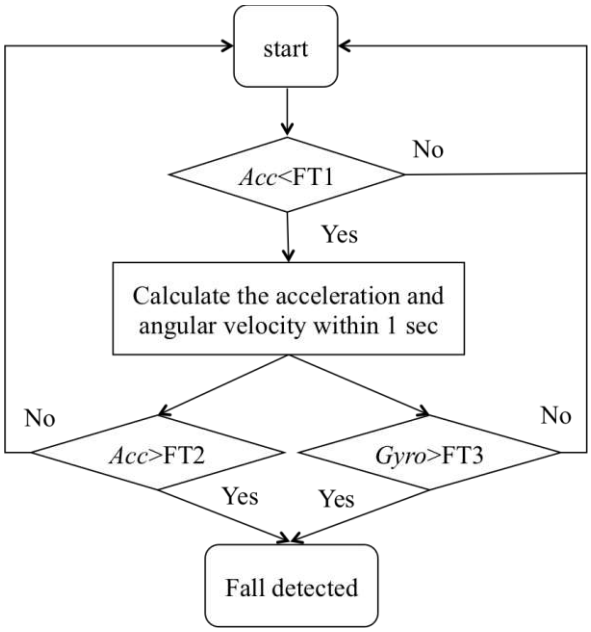

Fig. 2. The flow chart of fall algorithm using these threshold sets.

In this study, we use both FT1 and FT2 in combination with FT3 to detect fall event. All thresholds were determined by the the average values of all simulated falls and ADLs. Our proposed algorithm is shown in Fig. 2. When *Acc* value falls below the FT1 threshold, data from the next 1 sec are compared to FT2 and FT3 for *Acc* and *gyro* values, respectively. Within this period, if both *Acc* and *gyro* values are higher than FT2 and FT3, a fall event was detected. If only one or neither is observed, a fall event is not indicated.

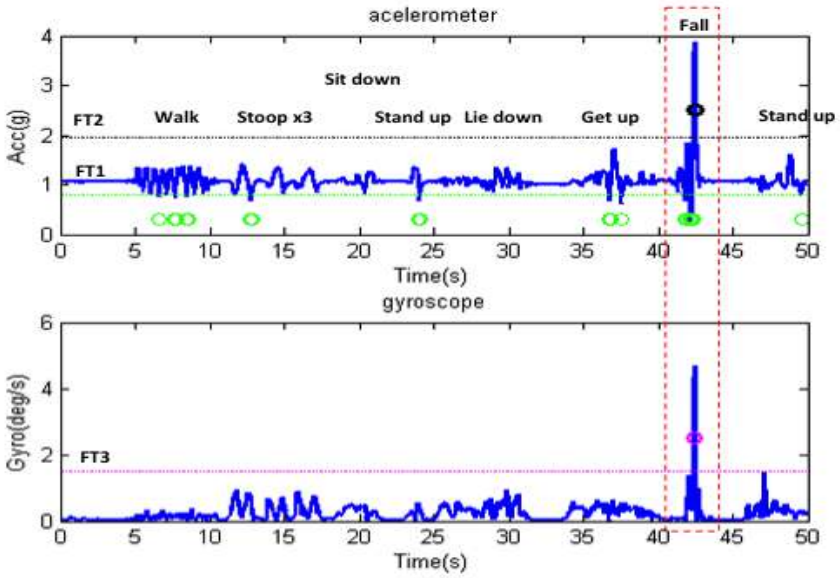

Fig. 3. Display of *Acc* and *gyro* for various activities: walking, stooping, sitting down, standing up, lying down, getting up, and forward falling. Also the thresholds of FT1 (green line), FT2 (block line), and FT3 (purple line) were set to determinate a fall event. Corresponding circle dots are the data points that upper and lower than thresholds. A fall event is indicated when FT2 and FT3 are detected within 1 sec after FT1 was detected (red square).

III. RESULTS AND DISCUSSION

Fig. 3 shows a typical example of *Acc* and *gyro* signals while wearing BC1 device and performing different daily activites and forword fall sequentially. Corresponding indications (circle) pointed out the *Acc* and *gyro* signals exceeds FT1, FT2, and FT3 during subjects performed different ADLs and simulated-fall. When the fall event occuring (at ~42 sec after recording), the Acc signal decreases from ~1 g to ~0.3 g to cross below FT1 (0.71 g). Then, whitin 1 sec, *Acc* and *gyro* signals increase to ~2.7 g and ~2.3 deg/s, respectively, to cross above FT2 (1.95 g) and FT3 (1.52 deg/s).

The *Acc* signal of some ADLs decresed below FT1 easily, such as stooping down, lying down, and getting up. The LPVs of *Acc* signal records from 6 subjects also indicated these (Fig. 4). However, the confirmatory FT2 are never reached at all ADL (Fig. 5). As previous studies, increasing acceleration was observed during a fall event because of the sudden body inertial changes [8]. We also found that the largely increasing acceleration at 8 simulated-falls. At the angular velocity, only the movement of lying down leaded to increasing angular velocity and crossing above FT3. (Fig. 6) The increasing angular velocity during lie down is possible due to the height of our bed is only 15 cm, and then result in subject's movement similar to fall.

Although using acceleration magnitude alone is available to distinguish falls and ADL in our simulated conditions, using three thresholds to distinguish falls and ADL have been demonstrated higher specificity in many previous studies [8]. Herein, by combining FT1, FT2, and FT3, 100% specificity was obtained in our testing conditions.

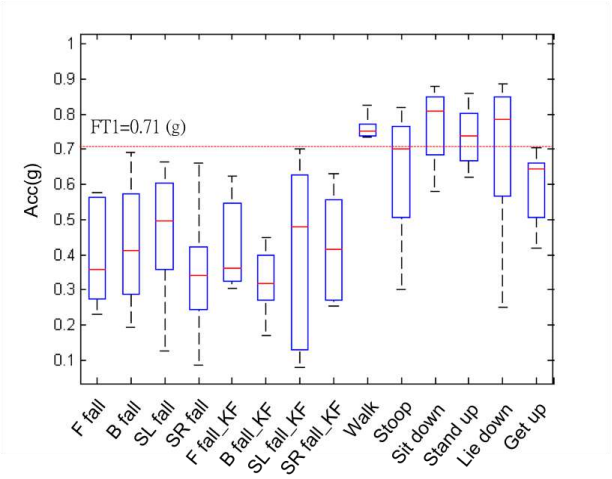

Fig. 4 Boxplot of LPVs for 8 types of simulated-fall and 6 types of different A DL. The red dot line is the FT1 value.

IV. CONCULSION AND FUTURE WORK

We have demonstrated that our wearable BC1 system is capable to detect falls automatically via this threshold-based algorithm. Currently, limited subjects were recruited and limited ADLs were performed in this work. For the optimization of this algorithm, a large number of subjects will be involved and analyzed. Also, different ADLs are also considered in the future.

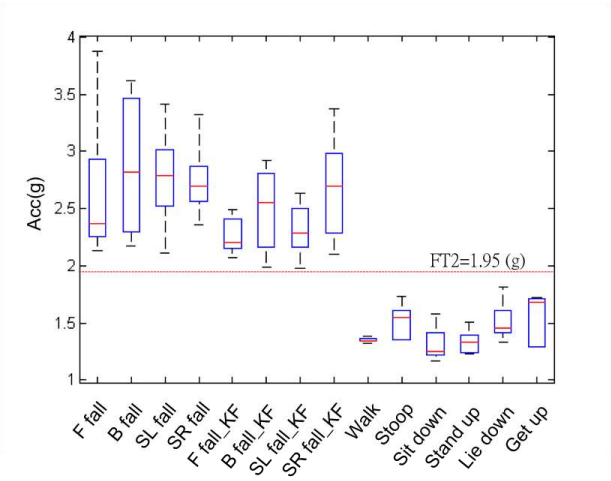

Fig. 5 Boxplot of LPVs for 8 types of simulated-fall and 6 types of different A DL. The red dot line is the FT2 value.

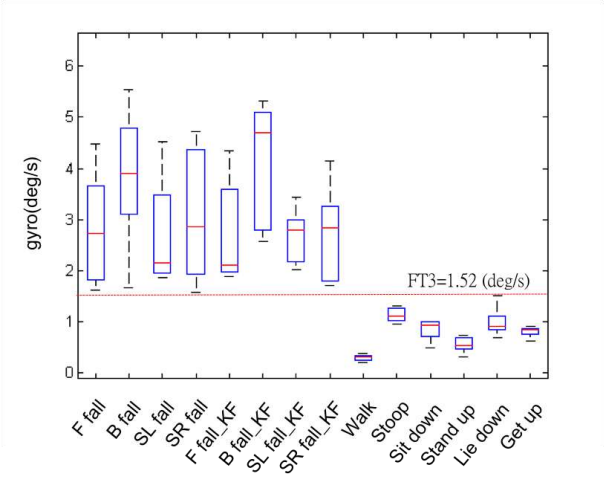

Fig. 6 Boxplot of LPVs for 8 types of simulated-fall and 6 types of different A DL. The red dot line is the FT3 value.

References

[1] J. Y. Hwang, J. M. Kang, and H. C. Kim J. Y. Hwang, J. M. Kang, and H. C. Kim, "Development of novel algorithm and real-time monitoring ambulatory system using bluetooth module for fall detection in the elderly," IEEE Engineering in Medicine and Biology Society, vol. 1, pp. 2204–2207, September 2004.

[2] National Center for Injury Prevention and Control and Centers for Disease Control and Prevention, *Cost of Falls among Older Adults*, National Center for Injury Prevention and Control, Centers for Disease Control and Prevention, 2013.

[3] J. Fleming and C. Brayne, "Inability to get up after falling, subsequent time on floor, and summoning help: prospective cohort study in people over 90," BritishMedical Journal, vol. 337, no. 7681, pp. 1279‑1282, 2008.

[4] D. Kunkel, R. M. Pickering, and A. M. Ashburn, "Comparison of retrospective interviews and prospective diaries to facilitate fall reports among people with stroke," Age and Ageing, vol. 40, no. 2, pp. 277‑280, 2011.

[5] E. M. Bertera, B. Q. Tran, E. M. Wuertz, and A. Bonner, "A study of the receptivity to telecare technology in a communitybased elderly minority population," Journal of Telemedicine and Telecare, vol. 13, no. 7, pp. 327‑332, 2007.

[6] N. Farber, D. Shinkle, J. Lynott, W. Fox-Grage, and R. Harrell, Aging in Place: A State Survey of Livability-Policies and Practices, AARP Public Policy Institute,Washington, DC, USA, 2011.

[7] L. Qiang, J. A. Stankovic, M. A. Hanson, A. T. Barth, J. Lach, and G. Zhou, "Accurate, Fast Fall Detection Using Gyroscopes and Accelerometer-Derived Posture Information," Wearable and Implantable Body Sensor Networks. Sixth International Workshop on pp.138,143, 3-5 June 2009.

[8] Quoc T. Huynh, Uyen D. Nguyen, Lucia B. Irazabal, Nazanin Ghassemian, and Binh Q. Tran, "Optimization of an Accelerometer and Gyroscope-Based Fall Detection Algorithm," Journal of Sensors, vol. 2015.

[9] B. J. Vellas, S. J. Wayne, P. J. Garry, and R. N. Baumgartner. "Atwo-year longitudinal study of falls in 482 community-dwelling elderly adults." J Gerontol A Biol Sci Med Sci 53(4):M264–74, 1998.

[10] C. Smeesters,W. C Hayes, and T. A. McMahon. "Disturbance type and gait speed affect fall direction and impact location." J Biomech 2001;34(3):309–17.

[11] A.K. Bourke, and G.M. Lyons, "A threshold-based fall-detection algorithm using a bi-axial gyroscope sensor," Medical Engineering & Physics 30:84–90, 2008.

5.

An Effective Algorithm for Dynamic Pedometer Calculation

An Effective Algorithm for Dynamic Pedometer Calculation

Jen Chien Chien, Koichi Hirakawa
Health and Beauty Research Center
Kinpo Inc.
New Taipei City, Taiwan

Han Wen Guo, Yita Hsieh
Health and Beauty Research Center
Cal-Comp Inc.
New Taipei City, Taiwan

Jiann-Shing Shieh
Dept. Mechanical Engineering
Yuan Ze University
Chung-Li, Taiwan

***Abstract*—The linear accelerometer is called G-Sensor. It supplies the information of accelerating change when some motion happens. The current G-Sensor products in the market are supported by 3-dimension information. The G-Sensor becomes the one of consumer components in this trend of MEMS technology development. The applications using G-Sensor components are working in the current market, for example, to be a way to control the game working, to control user interface, to drive some application programs or change slides by knocking the side of a device, to detect the falling event, and let hard disk inside the notebook have enough time to shutdown. And, G-Sensor can be implemented inside a pedometer. For wearable device, G-Sensor is used to the fitness application. The aim of this paper was to validate step counts and cadence calculations from acceleration data during dynamic activity. The proposed algorithm to calculate the accurate rate of dynamic step detection is 95%.**

Keywords—G-Sensor; acceleration; steps

I. INTRODUCTION

Obesity management for achieving an effective weight loss includes dietary modification and exercise [1]. Regular exercise is an effective method of weight loss and maintenance of weight. Exercise can prevent disease and maintain health. Therefore pedometers are often used as motivational tools to increase physical activity. Many previous studies have assessed the step count and gait event accuracy of pedometers, accelerometers, and gyroscopes [2–7]. Kenton compared commercial devices has the accuracy of 92% [8]. For these papers, they put the device on the waist. If the devices do not put on the waist, the accuracy must be decreased. We put our device on the chest, because our device has more functions that one is single lead ECG monitor and another is activity tracker (i.e., G-Sensor). We develop a simple and more effective algorithm to count steps and cadences.

II. METHOD

A. Data Collection

Six-axis sensor (Invensense MPU6500) was sampled to 100 Hz and calculated to steps by using a wearable G-sensor device (XYZ life BC1, Kinpo Inc., Taipei, Taiwan). The subjects wear a cloth with BC1 device, as shown in Fig. 1(A). The steps data was logged into a tablet PC via BC1 device shown in Fig. 1(B).

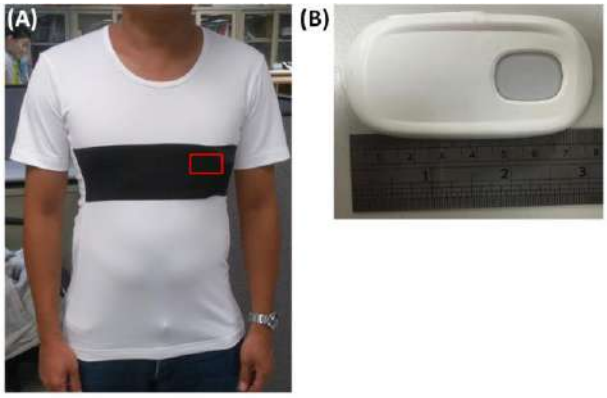

Fig. 1 (A) A fitting clothing with the BC1 device was used to collect the G-Sensor signals by the device placed in front of the left chest (red square). (B). The G-Sensor device BC1.

We collect five subjects walking data and set four kind of steps(50, 100, 300 and 500 steps). In order to avoid human counting errors, we use OMRON (Calori Scan HJA-310) to compare our device.

B. Algorithm Flow

We define the waveform of one step is like sine wave. And we define our algorithm as shown in Fig. 2. We use one sec data to set the calculating window. Firstly, we calculate 3-axis raw data to set data ACC where the equation is as shown in (1). Secondly, we take every two ACC to average. Third, we set the wave crest and wave trough candidate. Then, we can get the slope value. Fourth, if slope value is larger than threshold, the wave crest is large than ACC, and the wave trough is smaller than ACC, we consider that this is one step.

$$\mathrm{ACC} = \sqrt{\mathrm{X}^2 + \mathrm{Y}^2 + \mathrm{Z}^2} \qquad (1)$$

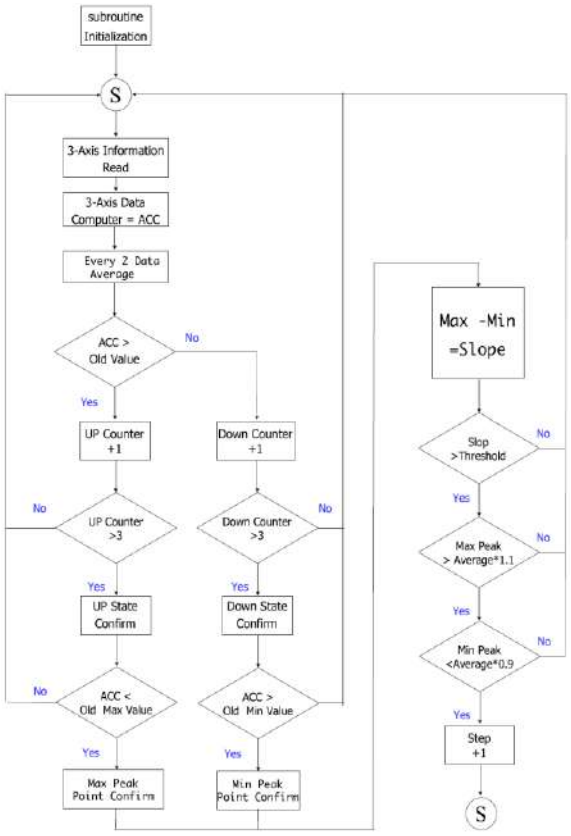

Fig. 2 This is the flow chart of calculating steps

III. RESULT

Table 1 is showed the error of step differnce between BC1 and real steps. According to the result, we can find the more steps which are smaller error values. But most of the pedometer are the more steps are bigger error values. Because we use dynamic windows that the average can be based on the step waveform to correct the value. For example, according to the Fig 3, these waveforms are to calculate the number of steps. Therefore, we must define what is "One Step". Fig. 3 is shown the three kinds of activity wave. These waveforms are very similar shape. And there are different with the detail data from G-Sensor value and frequency. We compare with the pick up as shown in Fig. 4 and walk. These waveforms pattern are different. So, the pick up is not calculated to step by our algorithm. The results suggest that the proposed analysis methods are suitable for step counting using tri-axial accelerometers on the chest in a free-living environment.

IV. CONCLUSION

In this paper, we develop a simple and more effective algorithm to count steps and cadences. The proposed algorithm to calculate the accurate rate of dynamic step detection is 95% when the step number is greater than 100 steps. It means that the proposed analysis methods are suitable for step counting using tri-axial accelerometers on the chest in a free-living environment.

TABLE I. ERROR STEP DIFFERENCE

Subjects	Steps			
	50	100	300	500
[A]	8%	5%	-0.3%	-1%
[B]	12%	0%	-1%	0.4%
[C]	8%	0%	0.3%	0.4%
[D]	4%	3%	0.7%	1.2%
[E]	-6%	1%	-0.3%	-0.2%
Mean	5.2%	1.8%	-0.12%	0.16%

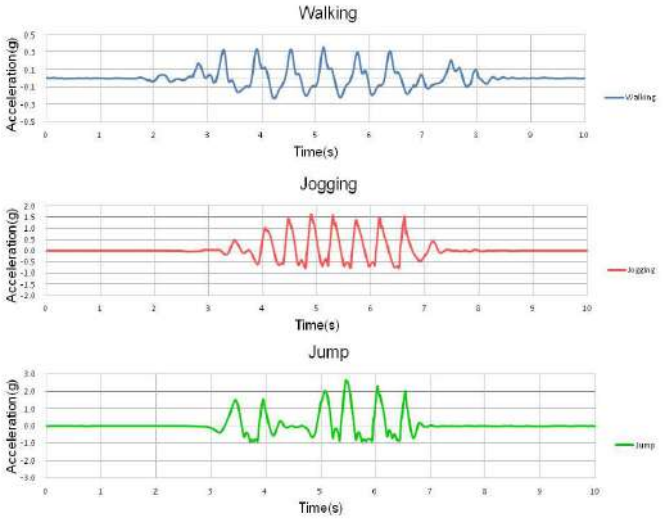

Fig 3. Three kinds of activity waveform

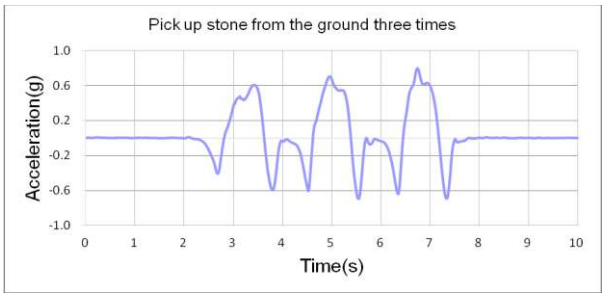

Fig. 4 The pick up waveform

Acknowledgement

This research was financially supported by the Kinpo Inc., New Taipei City, Taiwan. This research was also supported by the Health and Beauty Research Center of Kinpo Inc., New Taipei City, Taiwan.

References

[1] B. Bajer, M. Vlcek, A. Galusova, R. Imrich, A. Penesova, “Exercise associated hormonal signals as powerful determinants of an effective fat mass loss.”, Endocr Regul.,49(3):151-63., 2015

[2] SE. Crouter, PL. Schneider, M. Karabulut, Jr. Bassett DR., “Validity of 10 electronic pedometers for measuring steps, distance, and energy cost.” Medicine Science in Sports and Exercise., 35:1455–60., 2003

[3] DW. Esliger, A. Probert, SC. Gorber, S. Bryan, M. Laviolette, MS. Tremblay, ”Validity of the Actical accelerometer step-count function.”, Medicine and Science in Sports and Exercise., 39:1200–4., 2007

[4] Le. Masurier G., C. Tudor-Locke, “Comparison of pedometer and accelerometer accuracy under controlled conditions.”, Medicine and Science in Sports and Exercise., 35:867–71., 2003

[5] A. Salarian, H. Russmann, FJG. Vingerhoets, C. Dehollain, Y. Blanc, PR Burkhard, et al., “Gait assessment in Parkinson’s disease: Toward an ambulatory system for long-term monitoring.”, IEEE Trans Biomed Eng., 51:1434–43., 2004

[6] J. Rueterbories, EG. Spaich, B. Larsen, OK. Andersen, “Methods for gait event detection and analysis in ambulatory systems.”, Med Eng Phys., 32:545–52., 2010

[7] A. Mansfield, GM. Lyons, “The use of accelerometry to detect heel contact events for use as a sensor in FES assisted walking.”, Med Eng Phys., 25:879–85., 2003

[8] E. Fortune, V. Lugade, M. Morrow, and K. Kaufman, “Validity of Using Tri-Axial Accelerometers to Measure Human Movement – Part II: Step Counts at a Wide Range of Gait Velocities.”, Med Eng Phys., 36(6): 659–669., 2014